

Review

Phage-Based Sensors in Medicine: A Review

Sebastian J. Machera , Joanna Niedziółka-Jönsson  and Katarzyna Szot-Karpińska * 

Institute of Physical Chemistry, Polish Academy of Sciences, Kasprzaka 44/52, 01-224 Warsaw, Poland; sebastian.machera@interia.pl (S.J.M.); jniedziolka@ichf.edu.pl (J.N.-J.)

* Correspondence: kszot@ichf.edu.pl; Tel.: +48-22343-3130

Received: 1 June 2020; Accepted: 26 July 2020; Published: 31 July 2020



Abstract: Bacteriophages are interesting entities on the border of biology and chemistry. In nature, they are bacteria parasites, while, after genetic manipulation, they gain new properties, e.g., selectively binding proteins. Owing to this, they may be applied as recognition elements in biosensors. Combining bacteriophages with different transducers can then result in the development of innovative sensor designs that may revolutionize bioanalytics and improve the quality of medical services. Therefore, here, we review the use of bacteriophages, or peptides from bacteriophages, as new sensing elements for the recognition of biomarkers and the construction of the highly effective diagnostics tools.

Keywords: M13 bacteriophages; phage display; peptide; disease markers; molecular recognition; diagnostics; sensor

1. Introduction

Modern medicine has developed highly specialized techniques in order to diagnose diseases faster, cheaper and less invasively. In vivo imaging or body fluid (e.g., blood or urine) analysis lets specialists ‘take a look’ into the body and make conclusions as to both anatomical and physiological conditions of the whole organism. At the same time, significant progress in biochemistry has enabled recognition of novel bio-markers, i.e., substances whose abnormal level may be specific for some diseases [1]. For instance, increased levels of cardiac troponins in the blood is an integral part of the definition of myocardial infarction [2], while an increased level of alfa-fetoprotein in a pregnant woman’s blood or amniotic fluid may signalize severe fetal defects, such as spina bifida or evisceration [3].

Unfortunately, biochemical assays, e.g., enzyme-linked immunosorbent assay (ELISA), immunochromatography, flow cytometry, immunoturbidimetry, or real-time polymerase chain reaction (PCR) are mostly laboratory-use only because they can be expensive, time-consuming, and demand advanced laboratory equipment and experienced users. This limits their usage to hospitals or specialized institutions. To solve these inconveniences, a new generation of point-of-care tests (POC) is investigated and developed. A typical example of POC is a pregnancy test based on a lateral-flow immunochromatography test for human chorionic gonadotropin (hCG) [4]. This assay is based on monoclonal antibodies, which are known to be expensive and might be unstable [5]. Consequently, intensive studies were conducted to develop similar, easy and sensitive assays but using more stable and cheaper receptors, for instance, oligopeptides. Advanced molecular studies of antibody–antigen interaction showed that the binding of the antigen (i.e., the formation of the immunological complex) is determined by short peptide sequences characteristic for the antigen called ‘epitope’ [6]. Since it became clear that specific peptide–peptide interactions are one of the most essential life fundamentals, researchers have been making efforts to discover specific peptides that show high (similar to antibodies or even higher) affinity to the target. Very useful for these investigations is a technique invented by Smith in 1985 [7] called ‘phage display’ in which bacteriophages are used.

Bacteriophages (‘phages’) are viruses that infect bacteria. They are present in the soil, water and even in human intestines in great amounts [8–10]. They do not infect animals, but, moreover, they may

help them in controlling bacteria populations [9,11]. Interestingly, a decreased titer of phages in human feces may be connected with Leśniowski-Crohn disease according to their anti-inflammatory effect [9,11]. Phages may be easily genetically modified to display foreign peptide sequences on their coat proteins [12]. A pool of various variants of bacteriophages that display different foreign peptides is called a library. They are created by cloning foreign sequences directly into the phage protein gene (phage libraries) or into well-known places, i.e., multiple cloning sites recognized by various restriction enzymes in the additional part of a phage-genome-like plasmid (phagemid libraries). In the first case, all copies of phage proteins are modified, while the second one results in mosaic phage particles that contain both native and recombinant proteins or only recombinant, depending on phagemid and helper phage construction [13].

Desired variants of bacteriophages may be selected from a mixture of phage-displayed entities (e.g., affinity peptides or antibody domains) via affinity selection called ‘panning.’ This strategy mimics the natural process occurring when a human organism has contact with an antigen (i.e., a foreign protein). Antigen-presenting cells are able to display specific epitopes (i.e., 10–14 aa peptides) of foreign proteins, which may be bound by two types of lymphocytes B or T. The first ones are activated after binding and produce antibodies, while the second type after binding starts to kill pathogens. From the perspective of the whole organism, lymphocytes are tested for binding the antigen, and the binders are involved in an immunological response. The synthetic laboratory panning technique imitates this natural affinity selection. During the panning process, different binding domains (antibodies domains or peptides) are exposed on different phages, and the mixture is incubated with a functionalized target (immobilized or beads-coupled). Unbound individuals are washed out, whereas bound ones are eluted and sequenced to determine the sequence of the binding domain. The panning technique may be used for the direct evolution of proteins (e.g., enzymes) in the way resembling natural evolution. However, it takes a few hours—not millions of years [14].

Phage display has been applied in order to obtain or evolve antibodies, which was reviewed in detail in several publications [15–18]. Furthermore, recent reports describe the utilization of the phage display to investigate autoantibodies responsible for the development of some autoimmune diseases [19]. Phages also have a usage in treatment for drug delivery [20] and enzymes inhibitors’ generation [12,21]. Both wild-type and modified bacteriophages have a varied range of technical applications [22–28]. For medical diagnostics, the most important is phage display, which creates a new receptor for sensors. Depending on a type of transducer, we can divide sensors into several groups, such as electrochemical (voltammetric, potentiometric, impedimetric), optical (fluorescent, surface plasmon resonance, surface-enhanced Raman spectroscopy) and others, e.g., acoustic. In addition to genetically engineered bacteriophages, wild-type viruses were also applied in some sensing solutions, especially thanks to their natural affinity to host bacteria [29–32]. In this review, we would like to focus on the utilization of bacteriophages in medical diagnostics and show the most interesting and groundbreaking approaches.

2. Bacteriophages—Biology and Their Application in Phage Display Technology

Phages, like all viruses, consist of genetic material and protein capsid, which may take varied shapes, from the most recognizable rocket-like phage (T7 phage—in *Caudovirales* order) to icosahedral (Φ X174—in *Petitivirales* order) or a rod-like phage. In this review, we would like to focus on rod-like shaped phages called filamentous phages (Ff) belonging to the *Inovirus* genus in the *Inoviridae* family and *Tubulavirales* order [33], especially on M13 bacteriophage due to its further applications in molecular biology, e.g., the phage display technique. The M13 (as Ff type phage) has circular single-stranded DNA (ssDNA) that encodes 11 genes and simple intergenic regulatory sequences, the products of which are named pI (protein I) to pXI (protein XI); five of them (pIII, pVI, pVII, pVIII, pIX) are translated into structural proteins as the other six play roles during the replication of the phage [34]. In Figure 1, there is a scheme of M13 bacteriophage virion showing the localization of particular proteins. Ft phages are secreted from cell membrane without cell lysis or death, in comparison to lytic and lysogenic

virus lifecycles. The exact infection and amplification mechanism were reviewed and presented by Rakonjac et al. [34]. Briefly, infection of *E. coli* starts with the binding of F-pilus by pIII of the phage [35]. Then, its DNA is released into the cytoplasm and replicated. At the same time, some DNA copies are utilized for the synthesis of phage proteins. New virions are produced in the cell membrane by adding subsequent proteins to cover ssDNA. The process is finished by closing the capsid by pVI and pIII [34,36], so pIII is the first protein that attaches to the bacteria and the last one which leaves the host [37]. As the pIII is generally used for modification/displaying various motifs, a perturbation of its structure may have consequences for the efficiency of phage amplification [38]. The length of the phage particle is determined by the size/length of the pVIII [39,40]. In general, the wild-type M13 particle has 6.6 nm in diameter and about 800 nm in length [41].

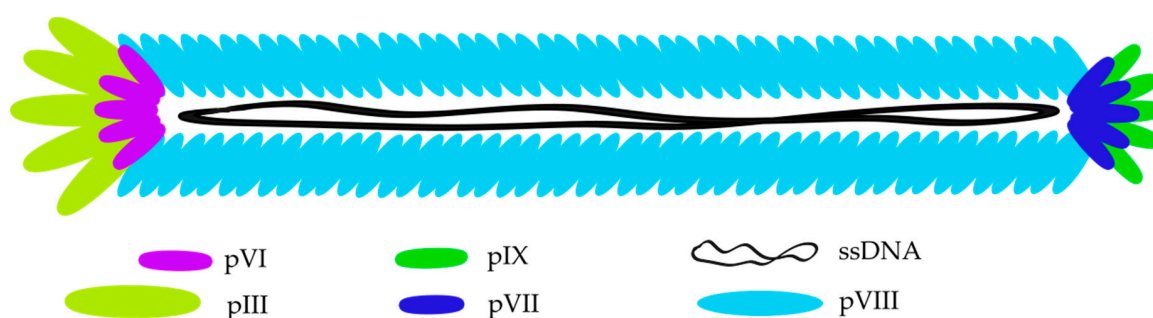


Figure 1. Scheme of M13 bacteriophage structure. Five types of coat proteins are presented with their localizations on phage particles but without a scale of proteins' size. The phage capsid covers single-stranded DNA and forms a rod-like structure 800 nm in length and 6.6 nm in diameter [41]. Wild-type M13 has approximately 5 copies of pIII, pVI, pVII and pIX coat proteins and about 2700 pVIII copies. Minor coat protein pIII is the biggest phage coat proteins and it allows the infection of cell host.

Thanks to the simplicity of the Ff phages, they were intensively studied since the 1970s. In 1985, G.P. Smith reported the first article that concerns the application of these phages—in the field later called *phage display* [7]. In turn, in 2018, he was awarded the Nobel Prize for developing this technique. Smith, in his pioneering work, incorporated a fragment of EcoRI (bacterial endonuclease—restriction enzyme) gene into the gene of the pIII of f1 bacteriophage. The obtained phages were harvested from *E. coli* culture and examined in terms of efficient displaying EcoRI motifs. As a result, the exposed on the phage capsid motif of EcoRI retains the ability to interact with specific antibodies while maintaining its infectivity [7].

Fusing foreign peptide sequences into a phage genome can be conducted in two general approaches. In the first one, DNA encoding desired gene is incorporated into the native phage protein gene. In a result, all copies of phage proteins are decorated with an additional fragment because the M13 genome consists of only one copy of every gene. The maximum size of the fused protein usually is expressed in the number of amino acids (aa)—described as capacity. This is connected with assembly and infection processes, e.g., for landscape library displaying peptide as long as 16 aa caused only 1% of phages survived [42] while pIII minor coat protein may carry almost 50 aa [43] or even 100 aa [44] depending on the study [45]. These size limitations can be overcome by a system called a phagemid ('phage and plasmid') [40]. Additionally, the application of the phagemid enables higher library diversity, but they demand an extra phage called 'helper phage' that produces native phage proteins necessary for replication [40,46].

Irrespective of the phage engineering method, libraries may be divided into two main types presented in Figure 2—pIII or pVIII ('landscape'), which are widely described in the literature [12,42,44,47,48].

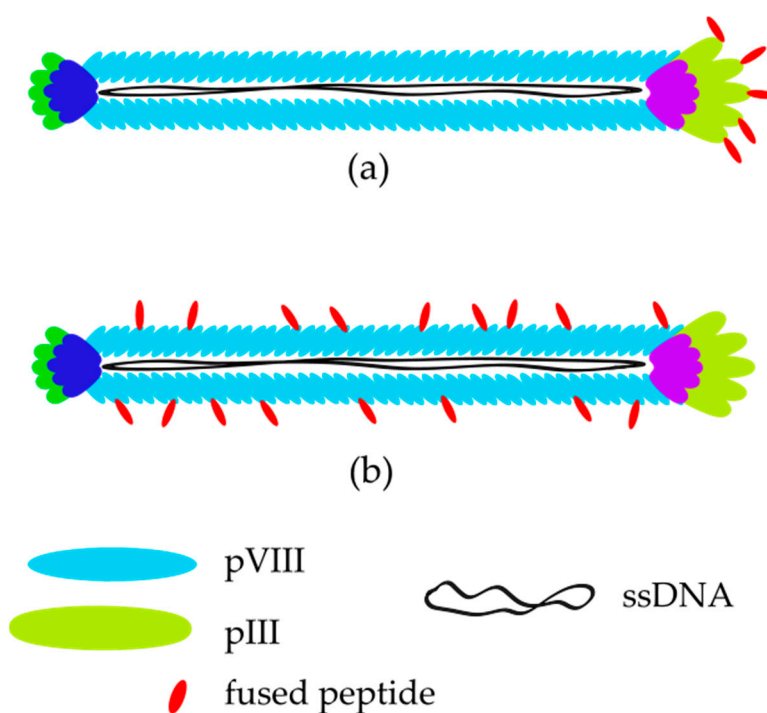


Figure 2. Most common types of phage peptide libraries: (a) peptide exposed on N-terminus (outer) of minor coat protein pIII and (b) peptide fused into some major coat protein pVIII (landscape library).

A comprehensive comparison of these two approaches was presented by Knez et al. [49] basing on affinity to enhance green fluorescent protein (eGFP) investigated kinetically via surface plasmon resonance (SPR) and enzyme-linked immunosorbent assay (ELISA). As a result, landscape (pVIII) peptides have a dissociation constant (K_d) three orders of magnitude lower than peptides exposed on pIII. The K_d value shows that interaction between eGFP and pIII is weaker than it is for pVIII. Because of methodological differences in experimental techniques, the results were consistent with the fact that landscape phages are more suitable for SPR because of the lower distance between bounded proteins and the surface of the sensor than to pIII-displaying ones that may be set perpendicularly to the sensor surface [49]. There is no clear evidence that shows that there is a difference in binding affinity between pVIII and pIII peptide system. However, it is known that landscape phages provide a higher number of affinity peptides.

Most of the experiments and research were conducted based on a commercially available Phage Display system (from New England Biolabs) [44]. Three offered systems: Ph.D.-7, Ph.D.-12 and Ph.D.-C7C provide linear 12 amino acid residues, linear 7 residues and cyclic (via cys-cys disulfide bond) 7 random residues peptides, respectively.

Molecular biology is an extremely dynamic field of research that causes an incredibly high number of modifications, improvements and applications of phage display. Therefore, we focus only on diagnostic applications of phage-displayed peptides as biosensing receptors.

3. M13 Bacteriophage-Based and Peptide-Based Sensors

Recently, novel label-free techniques that enable the direct detection of ligand-receptor interactions without any additional reagents, such as secondary antibody in immunological assays, have been a focus of research. Such biosensors are characterized by parameters such as sensitivity, selectivity, response time and additionally receptor affinity to the target (often shown by apparent dissociation constant, K_d). For phage-displayed peptides, the apparent dissociation constant is usually determined by the correlation of absorbance or fluorescence with the concentration of the incubated epitope-carrying

bacteriophages with the targeted molecule [50–52]. Additionally, apparent dissociation constant may be calculated from electrochemical impedance spectroscopy (EIS) by plotting relative resistance change against concentration [53]. In Table 1, we summarize several bacteriophage-based and peptide-based sensors detecting disease markers.

The main advantage of the application of phages and their peptides in the sensing systems is that they are less expensive in production and more stable to external factors such as temperature and various solvents than antibodies [54]. Owing to this, further modification through the conjugation of various functional groups is possible, which can be complicated with more delicate recognition elements. Additionally, the application of phages or peptides opens the possibility for the development of label-free assays.

There are a few reasons why we decided to describe only label-free sensors in this review. First of all, label-free technologies reduce the number of stages during measurements from two incubation stages (target binding and label binding) to only one (target binding). Consequently, the processing time is shortened, and the procedure is more straightforward than in labelled systems. On the other hand, there are some drawbacks and challenges that have to be overcome before introducing bacteriophage-based sensors into routine diagnostic procedures. The most serious difficulties are the calibration of the sensor (in case of reusable sensors) or repeatability of manufacturing (in case of disposable devices). The repeatability of the results is easier to achieve in the laboratory than in real-life circumstances where POC sensors are needed. However, thanks to the efforts of scientists, invented sensors are becoming more stable and accurate. Secondly, the receptor layer has to be resistant against external factors that may appear during sensor operation, e.g., vibrations, humidity differences or air pollutions etc. These obstacles have to be predicted by the researchers, described and/or solved at an early stage. At the end, manufacturing processes have to be optimized to minimize fabrication costs and labor without quality losses. Most of the mentioned difficulties are directly connected with the commercialization of the proposed sensing devices and may be some of the reasons why no phage-based sensor has been commercially available yet. Other causes might be connected with pejorative associations with viruses (even bacterial viruses), especially their safety both for people and the natural environment. There is a lot to do in the field of bacteriophage-based sensors; nevertheless, some excellent inventions have already been reported and highlighted in this work.

Table 1. Comparison of the bacteriophage-based and peptide-based sensors. Binding sequences do not include functionalizations of peptides such as cysteine or biotin.

Target	Binding Sequence	Affinity (Kd) ¹	Method	LOD	Reference
Whole M13 bacteriophage applied in sensor					
Prostate-specific membrane antigen (PSMA)	CALCEFGL	(n.a.)	QCM	(n.a.)	[55]
	CALCEFGL	(n.a.)	EIS	120 nM	
Prostate-specific antigen (PSA)	LDCVEVFQNSCDW	(n.a.)	VBR	100 pM	[56]
	ATRSANGM	(n.a.)	ELISA	1.6 ng/mL	
Human serum albumin (HSA)	(n.a.)	(n.a.)	DPV	3 pg/mL	[57,58]
			EIS	4 fg/mL (t-PSA)	
DJ-1 (bladder cancer marker)	KYRYVCHDVGTYCIRDGV	EIS: 300 nM (PBS)	VBR	100 nM	[59]
		EIS: 1036 nM (urine)		7.5 nM	[60]
Streptavidin (as a model protein)	ANRLPCHPQFPCTSHE	(n.a.)	VBR	10 pM	[61]
		14 pM or 206 nM		100 pM	[62]
Human phosphatase of regenerating liver-3 (hPRL-3)	(n.a.)	(n.a.)	OFRR	(n.a.)	[63]
			VBR		

Table 1. Cont.

Target	Binding Sequence	Affinity (Kd) ¹	Method	LOD	Reference
B-galactosidase	(n.a.)	SPR: 1.3 nM or 26 nM	SPR	(n.a.)	[64]
Dengue virus type 2 marker	EHDRMHAYLTR	EIS: 3.9 nM	EIS	0.025 µg/mL	[53]
Peptide-based sensors					
Troponin I (Tnl)	FYSHSFHENWPS	2.5 nM	EIS	0.34 µg/mL	[51,65]
		QCM: 17 nM and 66 nM	QCM	0.11 µg/mL	
Alanine aminotransferase (ALT)	WHWRNPDFWYLK	80 nM	EIS	92 ng/mL	[66]
			QCM	60 ng/mL	
Norovirus P2 protein	QHIMHLPHINTL	185 nM	EIS	99.8 ng/mL (P2) 7.8 virions/mL (whole <i>Norovirus</i>)	[67,68]
Myoglobin (Mb)	3R1: CNLSSSWIC	125 nM	DPV	3R7: 9.8 ng/mL	[69,70]
	3R7: CPSTLGASC	57 nM			
	3R10: CVPRLSAPC	293 nM			
Procalcitonin (proCT)	MSCAGHMCTRFV	1.9 nM EIS: 0.39 nM	EIS	12.5 ng/mL	[71,72]
Cholera toxin B	VQCRLGPPWCAK	6.7 nM	LSPR	1.89 ng/mL	[73]
			SERS	3.51 pg/mL	
Neutrophil gelatinase-associated lipocalin (NGAL)	DRWVARDPASIF	(n.a.)	SWV	3.93 ng/mL	[74]
			EIS	1.74 ng/mL	

¹—if it is not written otherwise, K_d was calculated from ELISA; abbreviations: n.a.—data not available, ELISA—enzyme-linked immunosorbent assay, LOD—limit of detection, EIS—electrochemical impedance spectroscopy, SWV—square-wave voltammetry, VBR—virus bioresistor, OFRR—optofluidic ring resonator, SPR—surface plasmon resonance, SERS—surface-enhanced Raman spectroscopy, LSPR—localized surface plasmon resonance, LAPS—light-addressable potentiometric sensor, QCM—quartz crystal microbalance.

3.1. Voltammetric and Impedimetric

In most cases, sensors based on voltammetry and electrochemical impedance spectroscopy (EIS) consist of an electrode coated with bacteriophages displaying affinity peptide or synthesized peptide as a receptor layer. Prostate-specific membrane antigen (PSMA) is a biomarker of prostate cancer and is overproduced in cancer cells and released to the prostatic part of the urethra so that it may be detected in urine or semen. In comparison to another tissue-specific protein, prostate-specific antigen (PSA), PSMA shows higher specificity to prostate cancer and is more suitable for diagnosis and prognosis [75]. One of the first virus-based sensors was proposed by Yang et al. [55]. In their work, M13 bacteriophages displaying a PSMA-binding sequence on the N-terminus of pVIII coat protein (established to be CALCEFLG) were immobilized on the surface of a gold electrode via an N-hydroxysuccinimide thioctic ester (NHS-TE) linker and monitored by quartz crystal microbalance (QCM) and EIS (Figure 3). The most time-consuming stage of PSMA concentration measurements using this sensor was incubation that lasted 1 h. The sensor was shown to have a limit of detection (LOD) of 120 nM (comparable to the normal level of PSMA) and also good stability for three binding/elution (pH = 2.0) cycles.

The work presented in [57,58] describes how the library of octapeptides fused into pVIII (landscape library) was screened against prostate-specific antigen (PSA), a biomarker of prostate carcinoma. Selected phage clone displaying PSA-binding peptide (ATRSANGM) was covalently immobilized to a mercaptopropionic acid (MPA) self-assembled monolayer (SAM) modified gold electrode surface. The analysis of the obtained electrode was performed via differential pulse voltammetry (DPV) and showed the LOD as low as 3 pg/mL [57]. Further research [58] performed with the same phage clone by EIS results in extremely low LOD (4 fg/mL for total PSA) (Figure 4). Moreover, thanks to the receptor layer construction, it was possible to obtain an electrode that was reusable after acidic elution (up to

6 rounds). These marvellous parameters of the sensor were obtained thanks to a dense receptor layer provided by landscape library and high sensitivity of EIS [58,76].

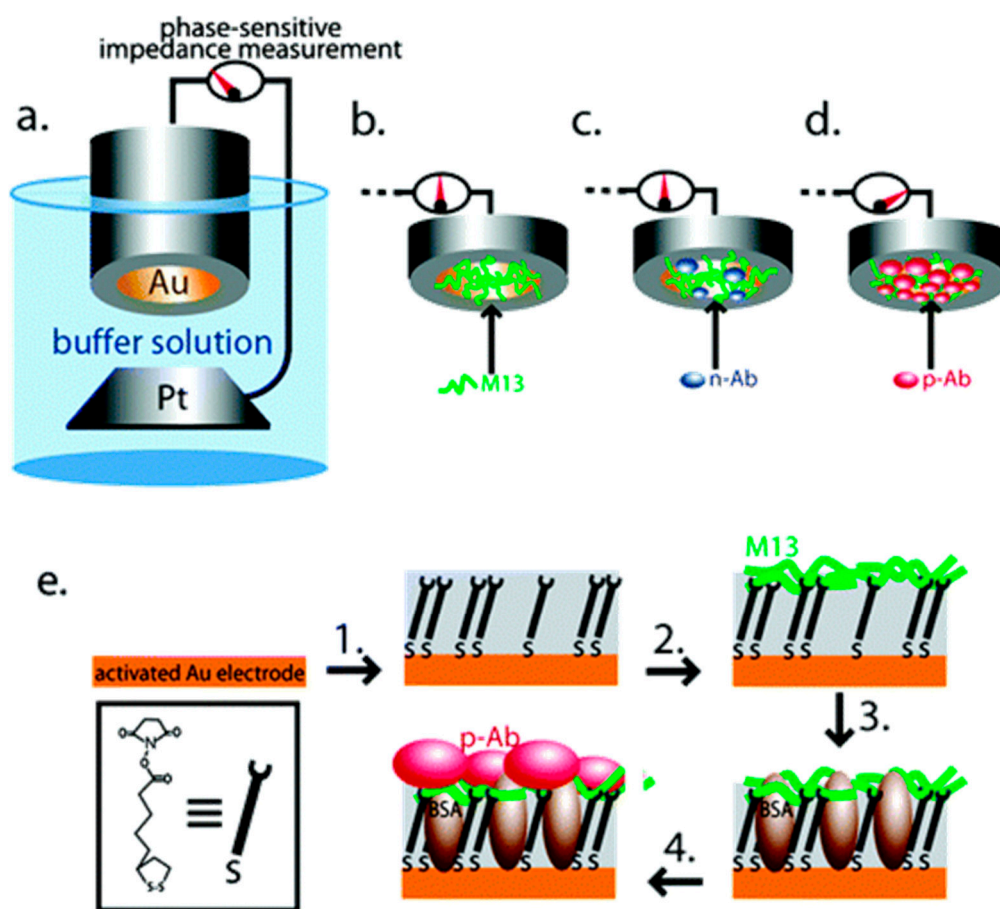


Figure 3. Scheme of a virus-based electrochemical sensor. Scheme of the measuring system (a) and reference state of the M13 virus-based electrode (b). The surface of a gold electrode is functionalized according to (e) 1–3. Sensor response (measured via EIS) is specified to the target—positive antibody, p-Ab (d)—and is negligible for a non-specific target—negative antibody, n-Ab (c). Reprinted with permission from [55]. Copyright 2006 American Chemical Society.

An analogous scheme was used for detection of the Dengue virus type 2 marker (DENV2 NS1 protein) [53]. A random 12-residues peptide library (Ph.D.-12) was screened and the binding clones were collected and characterized. Calculations of K_d was conducted not from indirect ELISA but using direct EIS measurement based on whole M13 phages immobilized on the electrode. For the finest peptide (EHDRMHAYYLTR) shown, $K_d = 3.9$ nM, while the whole electrochemical biosensor provided an LOD of 0.025 $\mu\text{g/mL}$. The obtained result is far lower than the level of viral proteins in patients' bloodstream (about 50 $\mu\text{g/mL}$) [53].

The construction of whole-phage biosensors promises the development of novel label-free and selective methods of point-of-care diagnostics. Moreover, phage amplification is less expensive and easier than the monoclonal antibodies production.

The preparation of a peptide-based biosensor contains two main stages: receptor selection (via phage display) and functionalization of a transducer with synthetic peptides. This approach was used to develop sensors for detection of troponin I [51,65], myoglobin [69,70], alanine aminotransferase [66] or *Norovirus* coat protein [67,68].

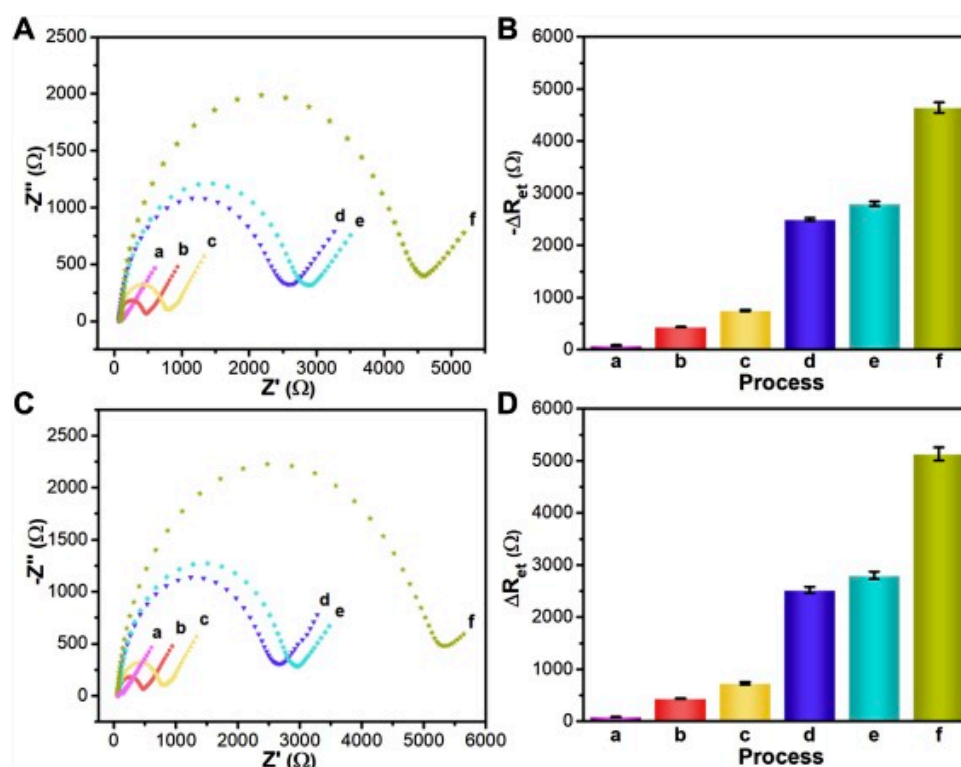


Figure 4. Impedimetric prostate-specific membrane antigen (PSMA) sensor fabrication (a–e) and operation (f): Nyquist plots (A), (C) and corresponding charge transfer resistance calculated using the alternative circuit. (A,B) correspond to one specific phage clone, whereas (C,D) present result for another phage clone applied in the sensor. Reprinted from [58], Copyright 2019, with permission from Elsevier.

Troponin I (TnI) participates in muscle contraction. It is important to note that the variant of TnI present in myocardium varies from its analogue from skeletal muscles thanks to alternative splicing and posttranslational modifications. After myocardial infarction, the concentration of TnI, is increasing quickly in the blood, and that can be measured [77]. For TnI, the 99th percentile threshold required by myocardial infarction definition [2] is between 0.01 and 0.07 $\mu\text{g/mL}$ depending on the method and assay manufacturer [78]. In order to construct an electrochemical sensor, firstly a TnI-binding peptide was selected and characterized by Park et al. [51]. For the panning stage, a commercially available pIII Ph.D.-12 was used. Clones displaying peptides with the highest affinity were chosen for characterization via ELISA and indirect ELISA. An apparent dissociation constant, K_d , was calculated according to modified Figuret's protocol of indirect ELISA [50]. Obtained peptide ligand (FYSHSFHENWPS) showed an apparent K_d at the level of 2.5 nM. Later, an electrochemical sensor based on this peptide was developed [65]. The affinity peptides labelled with cysteine were immobilized on the surface of a gold electrode via Au-S self-assembled covalent bond (Figure 5).

TnI detection was performed by EIS and quartz crystal microbalance (QCM). LODs were calculated to equal 0.11 $\mu\text{g/mL}$ and 0.34 $\mu\text{g/mL}$ for QCM and EIS, respectively. However, QCM kinetics experiments shown kinetic K_d for TnI-isolated peptide complex of 17 nM (direct kinetic measurements) and 66 nM (equilibrium plateau analysis) that is one order of magnitude higher than calculated from indirect ELISA [51,65].

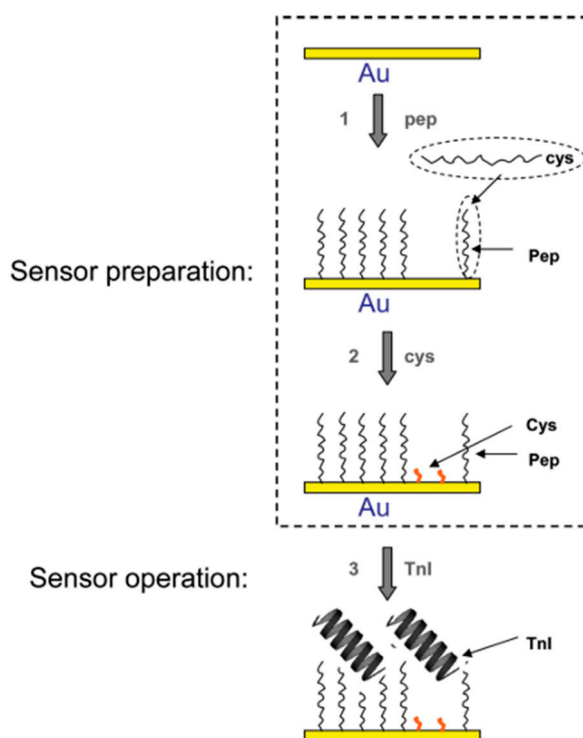


Figure 5. Scheme of peptide-based electrochemical sensor construction basing on a troponin I (Tnl) sensor. Subsequent stages include: (1) the immobilization of cysteine-labeled affinity peptides and (2) blocking with cysteine. Operation of the sensor consists of incubation with the target's solution (3) and electrochemical measurement in the electroactive depolarizer solution. Reprinted with permission from [65]. Copyright 2010 American Chemical Society.

An almost identical approach was applied in the construction of alanine aminotransferase (ALT) electrochemical biosensor [66]. This enzyme is found in the blood at the level between 0.1–0.7 mg/mL. Its concentration rises when the liver is damaged. ALT-binding peptide (WHWRNPDFWYLKC) was selected via panning from the Ph.D.-12 library. Apparent K_d (calculated from indirect ELISA) for peptide remained on pIII of the phage was 80 nM. The sensor was constructed identically as for troponin I [65], i.e., by chemisorption of cysteine-labeled peptides. The ALT sensor showed good parameters with LOD of 92 ng/mL for EIS and 60 ng/mL for QCM. Additional QCM kinetics assays showed kinetics, K_d , of the peptide on the electrode to be 20 nM [66].

A peptide-based human norovirus sensor was also constructed according to the above procedures [67,68]. Norovirus is a virus that infects humans and causes diarrhoea and other digestive system infection symptoms. On the virion structure, there is a protein called by the authors 'P2' and 'rP2' for native P-domain norovirus capsid protein and recombinant one, respectively. This well-exposed protein on the virion surface may be recognized by affinity peptide. For sensor construction, the M13 bacteriophage library (Ph.D.-12) was panned against recombinant norovirus protein rP2 [67]. The best binding sequence was found to be QHIMHLPHINTL (for rP2 protein), and K_d from ELISA was calculated to be 185 nM. Afterwards, this linear peptide was incubated on a clean gold electrode surface to obtain a self-assembled receptor layer [68]. This simple electrochemical sensor was able to detect recombinant norovirus protein and real sample norovirus particles with LOD at the level of 99.8 nM or 7.8 virus copies/mL, respectively. The difference might be easily connected with the size difference between isolated protein and whole norovirus size.

Myoglobin (Mb) is one of the myocardial infarction biomarkers, so measuring its concentration may be part of heart attack diagnosis [79]. A peptide library containing a random sequence of seven amino acids bordered by cysteine residues fused to the pIII minor coat protein of M13 bacteriophage

(Ph.D.-C7C system) was screened in order to select Mb-binding sequence [69]. After several panning rounds, three peptides were isolated: 3R1 (CNLSSSWIC), 3R7 (CPSTLGASC), and 3R10 (CVPRLSAPC) with K_d values: 125, 57 and 293 nM, respectively. Peptide–antibody and peptide–peptide assays are consistent with commercial kits results and an LOD as low as 25 ng/mL. However, the method was very time consuming and took 2–4 h. Afterwards, Mb-binding bisulfide-bonded 3R7 peptide (CPSTLGASC) [69] was immobilized on a dithiobis(succinimidyl propionate) (DSP) self-assembled monolayer (SAM)-modified gold electrode [70]. The obtained electrochemical sensor was examined using cyclic voltammetry (CV) and differential pulse voltammetry (DPV). In comparison to the ELISA test performed with the same peptide, electrochemical sensors showed a lower LOD (9.8 ng/mL) and a fast response time of about 30 min [70]. This example greatly highlights advances of label-free electrochemical sensors in comparison to previous antibody-based immunoassays.

Procalcitonin (ProCT) is a sepsis marker [71,72]. A 12-mer random peptide library (Ph.D.-12) was screened to select a ProCT-binding peptide. After several rounds of panning, a phage clone carrying the consensus sequence MSCAGHMCTRFV was isolated and characterized via ELISA. Calculated from the experiments K_d equals 1.9 nM in PBS, while the addition of serum caused a decrease in binding efficiency [71]. Furthermore, the affinity peptide was chemically synthesized with a flexible linker (GGGS) and C-terminal cysteine [72]. ProCT-binding peptides were chemisorbed on the surface of a gold electrode. All stages of sensor construction and operation were investigated via electrochemical measurements. The impedimetric measurements show that K_d measured for the isolated peptide immobilized on the gold surface is considerably lower than for the peptide exposed on phage coat protein and was calculated as 0.39 nM [72].

Later, Cho et al. constructed a peptide-based electrochemical sensor for the detection of neutrophil gelatinase-associated lipocalin (NGAL)—a marker of acute kidney injury [74]. By panning the peptide library (Ph.D.-12 system), the best binding sequence (DRWARDPASIF) was selected and chemically synthesized including -GGGSC label at the C-terminus. In addition, NGAL-binding peptide analogues such as reverse sequence peptide (FISAPDRAVWRD), modified (KRWVAKDPASIF) and doubled (DRWVARDPASIFDRWVARDPASIF) were studied to potentially be used in NGAL sensors. The experiments show that the basic sequence (DRWARDPASIF) gave the highest affinity and was used for sensor investigation. Affinity peptides' immobilization was performed by the formation of 11-mercaptoundecanoic acid (MUA) self-assembled monolayer, and further immobilization of peptides using activation of MUA carboxyl groups by EDC (1-ethyl-3-(3-dimethylaminopropyl)carbodiimide). The constructed sensor was examined to detect various concentrations of NGAL in the range 0.0001 to 7.5 µg/mL using EIS and square-wave voltammetry (SWV). The response of the sensor was more linear for EIS than for SWV measurements. The LOD was determined to be 1.74 ng/mL and 3.93 ng/mL for EIS and SWV, respectively [74].

For these simple peptide-based sensors, receptor density is defined as the density of affinity peptide SAM, which was measured by QCM to be (in cm^{-2}) 1.214×10^{12} , 7.4×10^{13} and 1.27×10^{15} [65,68,80], respectively.

3.2. Virus Bio-Resistor (VBR) Sensing Devices

The term 'virus bio-resistor' (VBR) refers to a device that contains virus particles (e.g., M13 bacteriophages) directly connected with the electric circuit. Predominantly, VBRs are constructed by assembling virus particles in poly(3,4-ethylenedioxythiophene)—PEDOT. This electrically conductive polymer forms positively charged dimensional structures during electropolymerization, i.e., the process of polymerization connected with redox reaction (Figure 6). The PEDOT layer usually envelopes negatively charged ions; however, in VBRs, the virus particles are used as negatively charged individuals [80]. Virus bio-resistor is a relatively new approach for sensor construction, which is connected with a stable interest in phage display. The VBR sensor constructed by the immobilization of M13 phages in the PEDOT layer was first examined for binding of anti-M13 antibodies. The impedance measurements show that charge transfer resistance increases with an increasing concentration of

specific antibodies. Secondly, the VBR sensor was studied in the presence of the non-specific antibodies. The results show that the binding of non-specific entities is minimal and almost concentration independent [80,81].

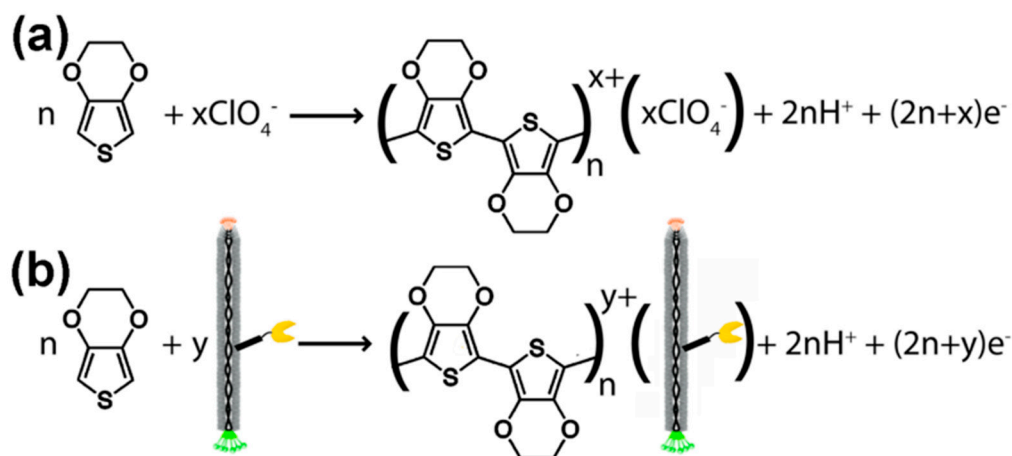


Figure 6. Scheme of the electropolymerization of EDOT (3,4-ethylenedioxythiophene) (a) in LiClO₄ and (b) in phage solution. Both negatively charged individuals are embedded in the polymer structure. The yellow ‘pacman’ symbolizes PSMA-binding peptide exposed on the pVIII major coat protein of phage. Reprinted with permission from [82]. Copyright 2012 American Chemical Society.

Since initial descriptions of M13 bacteriophage embedded into the PEDOT ultra-thin layer, several sensing [56,59,61,80–83] devices were constructed and examined. First, a VBR point-of-proof biosensor was constructed using a modified PSMA-binding peptide reported previously (LDCVEVFQNSCDW) [55]. Briefly, a gene fragment was selectively mutated and the mutants were panned against PSMA in a process called affinity maturation. Novel peptide (SECVEVFQNSCDW) has two N-terminal (outer) residues mutated and shown a higher affinity to PSMA dimer (>100-fold increase in comparison to unmutated peptide [82]). After the deposition of M13 phages displaying PSMA-binding sequences, target detection was monitored by EIS and shown LOD as 56 nM (5.6 µg/mL). The synergic approach was proposed by Mohan et al. [56], who applied both PSMA-binding peptides selected by Yang: PSMA-1 (CALCEFLG) and PSMA-2 (LDCVEVFQNSCDW) [55]. Here, the M13 phage displaying one PSMA-binding peptide was chemically modified using the second sequence (Figure 7). Hence, a hybrid phage-based receptor layer was established. The authors proved that the best results were obtained when PSMA-2 peptide was fused into pVIII protein, and PSMA-1 was added via chemical modifications. This comprehensive research allows for the lowering of the LOD to 100 pM (in synthetic urine) and 3.1 nM in PBF (phosphate-buffered fluoride) [56], which is 2 or 3 orders of magnitude lower than that reported for the previous VBR biosensor [82].

Later, a virus-PEDOT impedimetric sensor was investigated to detect human serum albumin (HSA), which appears in the urine, the kidneys or bladder diseases [59]. The authors constructed their phagemid library—a mega random peptide library. It contains a random peptide sequence from 5 to 18 amino acids and provides a tremendous diversity of displayed peptides [59]. Peptides selected from this pool of ligands were screened and characterized. The best HSA-binding sequence was established to have K_d at the level of 45 nM (via ELISA) or 300 nM (PBS solution, measured via EIS of VBR) or 1036 nM (synthetic urine, measured via EIS of VBR). The good parameters of VBR (Figure 8) described above and a satisfying LOD as low as 100 nM show promise for utilization of that sensor in clinical investigations. Even better properties (higher signal-to-noise ratio, lower response time) were achieved for the next VBR sensor described by Bhasin et al. [60]. In their work, some improvements were applied, such as virus-PEDOT layer parameters. Additionally, a thorough analysis of the theoretical

aspects of virus bioresistors was presented. In a result, LOD was reduced to 7.5 nM for HSA detection with a response time of 3–30 s.

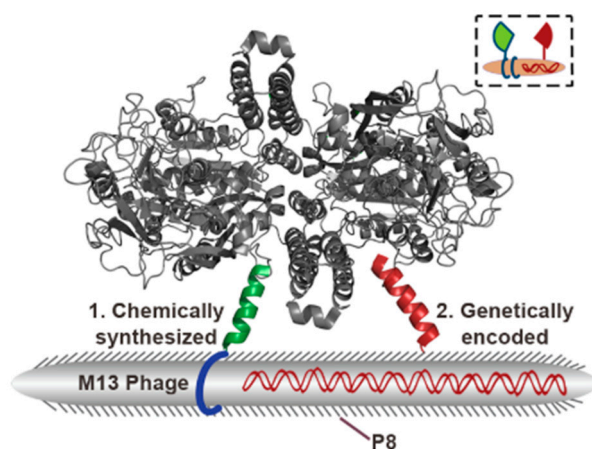


Figure 7. Scheme of a bifunctional M13 bacteriophage engineered to bind prostate-specific membrane antigen (PSMA). One peptide is fused into the pVIII major coat protein, while the second one is chemically bounded to phage particle [56]. Reprinted with permission from [56]. Copyright 2013 American Chemical Society.

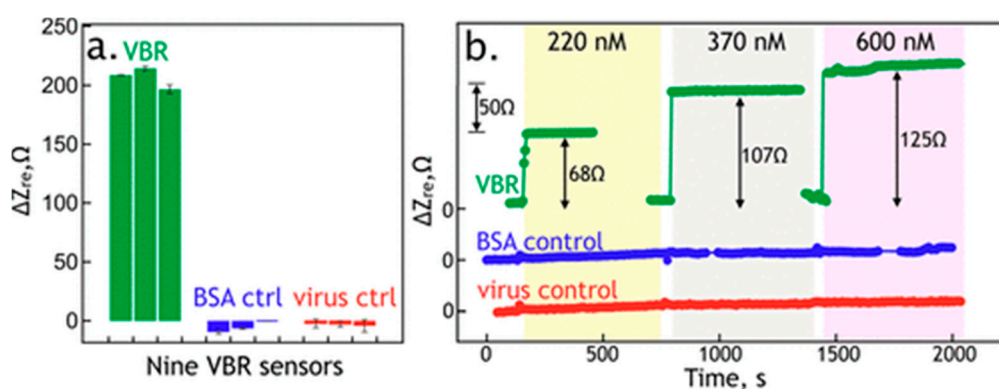


Figure 8. (a) Selectivity of the human serum albumin (HSA) virus bioresistor sensors against bovine serum albumin (BSA) (VBR sensor operated in a solution of BSA instead of HSA) and the control (PEDOT layer containing wild type phages do not bind HSA), (b) VBR sensor response (real impedance change) for varied HSA concentrations, control BSA probes and wild-type virus were applied as in (a). Reprinted with permission from [60]. Copyright 2018 American Chemical Society.

Recently, a novel VBR sensor for detection of DJ-1 protein—a marker of urinary bladder cancer has been presented [61]. The DJ-1-binding peptide was initially established to be KYRYVCHDVGGTYCIRD*V, where (*) means ATG codon (STOP codon—termination of protein biosynthesis). To obtain the specified peptide, direct mutagenesis was applied to replace STOP codon with CAG, which contains glycine, a simple amino acid). Modified peptide (KYRYVCHDVGGTYCIRLDGV) was displayed on pVIII major coat protein of M13 bacteriophage. Subsequently, the phages which display new peptide were incorporated into a virus-PEDOT layer of VBR sensor. The characterization of affinity peptide conducted via indirect ELISA protocol shown two apparent dissociation constants, 206 nM and 14 pM, for phage-covered and DJ-1-covered ELISA plates, respectively. Additional impedimetric measurements suggest K_d to be 39 nM. The LOD of the sensor was 10 pM [61].

3.3. Light Addressable Potentiometric Sensors

In contrast to previously described sensors, the light-addressable potentiometric sensors (LAPS) use potential value as a measurable chemical signal. This idea is based on measuring electrolyte-insulator-semiconductor system properties directly connected with a receptor layer state. Moreover, thanks to the fact that the charge current is caused by the excitation of semiconductor electrons with laser light, layer properties may be determined for different areas of the sensor [84]. In 2007, Jia et al. reported the construction of a groundbreaking phage-LAPS sensor for the detection of cancer cells and cancer biomarkers [63]. In their work, not only the affinity peptide was able to bind selectively to human phosphatase of regenerating liver-3 (hPLR-3) but also the human adenocarcinoma-binding sequence was selected via phage display from a commercially available peptide library (Ph.D.-12). Subsequently, M13 bacteriophages were immobilized on the surface of LAPS chip using APTES-glutaraldehyde functionalization [63]. Phage-LAPS examination showed that the detection of both hPLR-3 and adenocarcinoma cells is possible for concentrations of 40–400 nM and 10^3 – 10^5 cells/mL, respectively. However, LAPS was more sensitive for cells probably due to their size and electric properties in comparison to the hPLR-3 protein, which is smaller to the M13 phage and plays the role of the receptor [63].

3.4. Surface Plasmon Resonance and Surface-Enhanced Raman Spectroscopy Based on M13 Bacteriophage/Peptide Sensors

SPR enables real-time and label-free monitoring of interactions between individuals bound to a metal surface and free individuals present in the solution. Thanks to these handy advantages, SPR may be applied for kinetics measurements, e.g., the modelling of receptor–ligand complex creation or dissociation rates.

Despite several reports of usage of antibodies in SPR sensors [85,86], whole particles of genetically modified M13 bacteriophages were applied only in some proof-of-concept works. In one of them, *Salmonella*-binding M13 phages were selected from the phage library (Ph.D.-12) and covalently bound on dextran-modified gold chip [87]. The constructed sensor provides high selectivity for *Salmonella* and satisfying ability to detect 3 colony-forming units (CFU) of *Salmonella* in 25 g of the analyte [87]. Ding et al. presented a sensor for glyphosate that was based on a phage-displayed peptide [88] selected via phage display binding sequence (TPFDLRPSSDTR), which showed a $K_{app,d}$ of 8.6 μ M. Next, the peptide with a linking sequence (GGGC) at the C-terminus was immobilized on a gold SPR chip via cysteine–gold interaction. This simple method of sensor preparation gives result in a LOD = 0.58 μ M [88].

An excellent study of SERS applications in diagnostics was reviewed by Pilot et al. [89]. Moreover, M13 bacteriophages were applied in the development of SERS sensors. One of them may be used for detection of cholera infection. An affinity peptide for cholera toxin B was selected from 12-mer peptide library (on pIII of M13) [73]. Indirect ELISA has shown that the best binder (sequence: VQCRLGPPWCAK) has K_d = 6.7 nM. The peptides were immobilized on the surface of a glass–gold surface via cysteine–gold interaction. Sensor operation was examined using localized surface plasmon resonance (LSPR) and SERS; however, SERS was adjudged to be better for sensor development thanks to higher signal enhancement. The LODs were 1.89 ng/mL and 3.51 pg/mL for LSPR and SERS, respectively [73].

3.5. Virus-Based Colorimetric Sensors

A self-assembling M13 bacteriophage structure was intensively investigated both in technical and medical applications, which was greatly reviewed by Moon et al. [90]. Here, we would like to highlight sensing devices based on phage self-assembled structures that were examined to be potential diagnostics tools for varied (including medical) applications [91–98].

A proof-of-concept study was firstly reported by Oh et al. [91], who described (1) a humidity-dependent structure (and corresponding color) of the M13 phage layer, (2) volatile organic compounds'

impact on the M13 layer and (3) an ability to detect TNT (2,3,6-trinitrotoluene, an explosive agent). M13 phages are known to build different types of liquid crystalline structures that may be differentiated with a bare eye [99]. The type of the structure is determined during assembling by phage concentration and pulling speed [91,99]. What is essential for these studies, the structure of M13 layer is changeable and depends on solvents that may be explained by thickness changes that directly affect reflected light spectrum observed as color [91]. Detection using a phage-based colorimetric sensor is label-free, fast, and possible to conduct using an iPhone supplemented with an RGB analyzing tool [91].

The analogical approach was applied to construct phage-based colorimetric assay for endocrine-disrupting chemicals such as phenol, phthalic anhydride, or chlorobenzene derivatives or antibiotics [92,94]. As in previously described studies, WHW (a π interacting motif) was fused into pVIII major coat protein and phages were simply adsorbed on the platform surface according to Figure 9. Sensor examination has shown that, using the same sequence displayed on M13 phage particle, a high number of homologous chemicals may be distinguished and recognized due to the characteristic color change of particular bands on colorimetric sensor (Figure 10). The analysis may be easily monitored by amateur devices and programs [92,94]. Similar studies were presented by Kim et al. [98]. The authors presented a construction of a 9-chip colorimetric sensor that is able to recognize different estrogens (steroid hormones with homologous cholesterol-based molecular structure) or antibiotics. Wide analysis allows for preparation of a hierarchical dendrogram enabling summarization of sensor capabilities [98]. Tronolone et al. presented a protocol of electrical field assistance during phage layer assembly that reduces the time of colorimetric sensor preparation [97].



Figure 9. Scheme of phage-based colorimetric sensor preparation. M13 bacteriophages are engineered to display WHW (π aromatic interacting motif) on their pVIII major coat proteins. Subsequently, phages are pulled on the carrier to form a self-assembled structure [94]. Reprinted from [94], Copyright 2017, with permission from Elsevier.

3.6. Optofluidic Ring Resonator

Optofluidic ring resonator (OFRR) is a novel label-free optical sensing device based on the interaction of laser light with whispering gallery modes (WGMs), i.e., internal resonance mode extending between the inner surface (receptor layer) and outer border. A change in properties of a receptor layer causes a change in a refractory index, which is measurable [62,100,101]. The scheme of the OFRR system is presented in Figure 11. From bio-individuals for which OFRR sensors were constructed [101], two are connected with M13 bacteriophages. In the first, phages were detected by OFRR sensor functionalized with anti-M13 antibodies [100], while the second one presents genetically modified M13 phages that were applied as a receptor for streptavidin detection [62]. Both were real-time and label-free proof-of-concept works that show an opportunity to use OFRR sensors in point-of-care diagnostics. For the detection of streptavidin, C5R2 affinity peptide (ANRLPCHPQFPCTSHE) was applied. The sequence of that peptide was established via phage display library panning against streptavidin [102]. C5R2 phages displaying a streptavidin-binding sequence on pVIII major coat protein were immobilized on the inner surface of OFRR. The optical measurements show that C5R2

clones bind streptavidin more selectively and strongly than the negative control (phage displaying peptide without affinity to streptavidin). In turn, concentration-dependent measurements enabled the calculation of an apparent dissociation constant according to the methods presented by Petrenko and Vodyanoy [52]; K_d was found to be 25 pM [62]. On the other hand, the regeneration of the receptor layer was impossible as bare capillary was reusable when it was cleaned and immersed in HF [62].

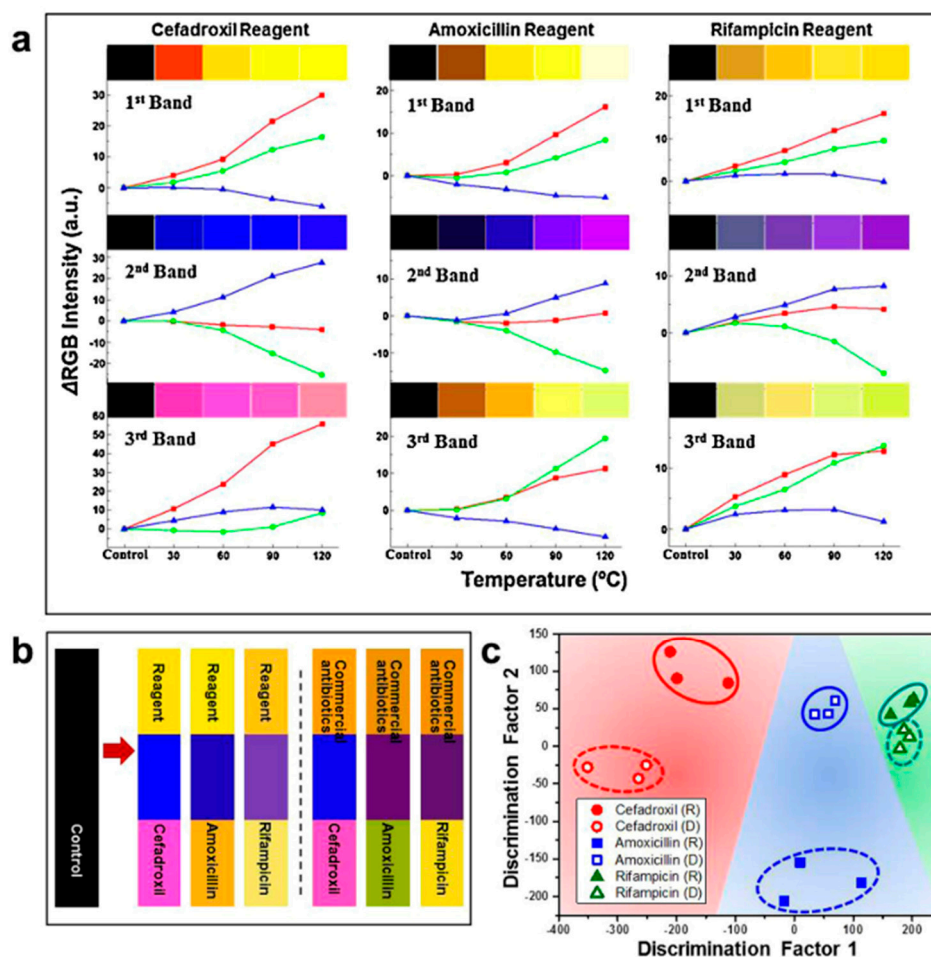


Figure 10. Each analyte (here three antibiotics) causes a unique color pattern that is highly temperature-dependent (a). Phage-based colorimetric sensors enable recognition of pure antibiotics from each other and a pure antibiotic from a commercially available form (with additional substances that interact with M13 structure) (b). Two-dimensional color pattern presentation shows a characteristic distribution of measured signals. Pure antibiotics (fulfilled signs) and their commercial forms (hollow signs) may be easily recognized with good accuracy (c) [94]. Reprinted from [94], Copyright 2017, with permission from Elsevier.

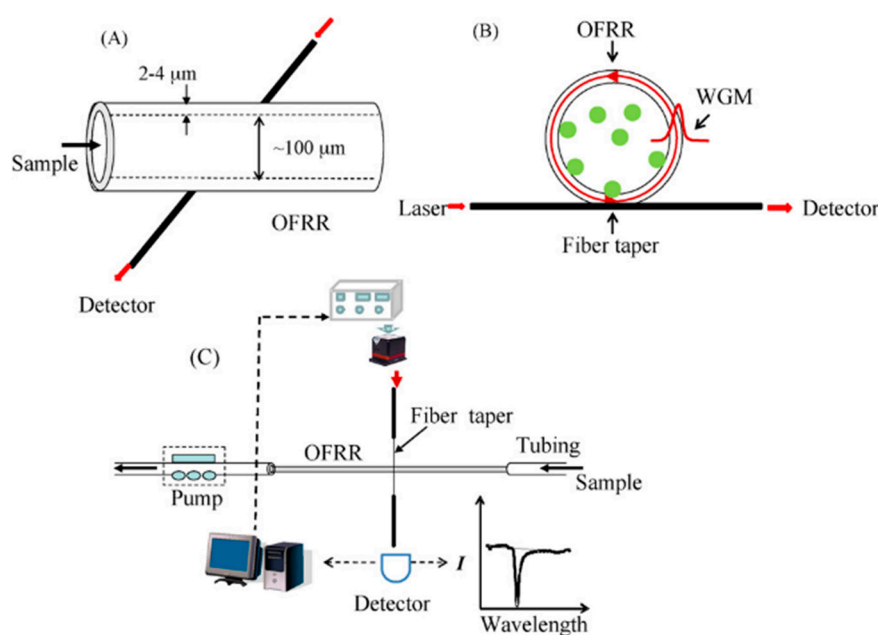


Figure 11. Scheme of optofluidic ring resonator (OFRR) sensor. (A) OFRR consists of a glass capillary with an ultra-thin wall (2–4 nm) and lumen about 100 μm in diameter. (B) Whispering gallery modes (WGMs) may be investigated by a laser directed on the OFRR. (C) Schematic of the apparatus required to run an OFRR sensor. [62] Reprinted from [62], Copyright 2008, with permission from Elsevier.

4. In Vivo Imaging by M13-Labeling of Cells

M13 bacteriophages are unique individuals which are able to simultaneously carry affinity peptides and chemical labels such as fluorescent dyes or nanoparticles [103]. These specialized viruses may play a role of highly selective labelling agent, e.g., for selective staining in histology [104]. In order to perform this advanced phage-based cell labeling system, a specific peptide-carrying phage must be additionally modified by adding the second peptide, which, e.g., binds nanoparticles or is conjugated with fluorophores. Selecting cell-specific peptides is possible thanks to the presence of specific cell receptors exposed on the cell membrane. Biopanning against eukaryotic cells may be conducted almost identically as for protein molecules. A comprehensive overview of cell-specific peptides obtained via phage display was presented by Xu et al. [105].

Research showing a general idea of a phage-based labeling system was performed by Kelly et al. [106]. Firstly, M13 bacteriophage clone displaying peptide-binding secreted protein acidic and rich in cysteine (SPARC)—a molecular marker of developing tumor—was isolated from the Ph.D.-7 peptide library (seven amino acids fusion on pIII) while vascular cell adhesion molecule-1 (VCAM-1) binding peptide (SPPTGIN) was selected from the Ph.D.-C7C circular heptamer library. Both peptides were identified according to standard protocols of *in vitro* panning against the pure protein. Further analysis showed the sequence of the SPARC-binding peptide to be CVHSPNKKC (the strongest binding shown by ELISA) [106]. Furthermore, SPARC-binding M13 clone coupled with fluorophores was examined to bind *in vivo* mice fibroblasts culture (against the negative control of the cell line without an SPARC-encoding gene). Moreover, *in vivo* labeling was also performed. Both analyses have shown great results, especially high selectivity and an ability of a labeling system to operate in living organisms [106]. Figure 12 shows labeling of cancer cells by SPARC-binding virions visualized using fluorescent molecular tomography. Additionally, penetration of phage was observed, which may be important for drug delivery via phage systems. Moreover, VCAM-1 binding phage may be used in immunohistological studies. High-affinity peptide exposed on M13 particle enabled differentiation of vessels expressing VCAM-1 from not expressing this factor [106].

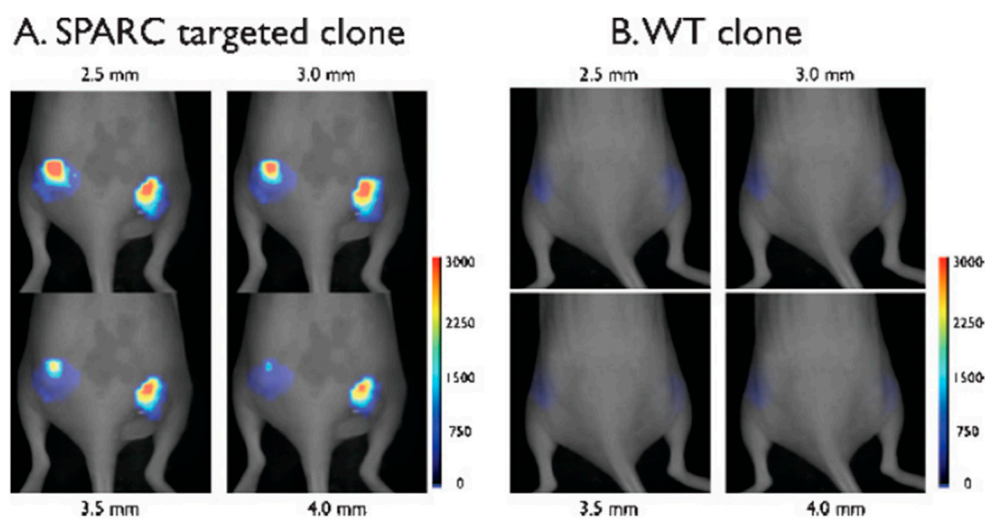


Figure 12. In vivo fluorescent labeling of tumors in mice thanks to modified M13 bacteriophages (A) and negative control wild-type phage (B) [106]. Reprinted from [106], Copyright 2006, with permission from Elsevier.

The method described above was based on displaying one fusion on phage coat proteins. However, there is a second approach that utilizes biofunctionalized bacteriophages. According to the work of Ghosh et al. [107], M13 phages may carry two specific peptides; the first peptide is cell-specific (on pIII minor coat protein), while the second is fused to pVIII major coat protein and binds iron oxide nanoparticles. The in vivo imaging technique is performed on mice, which are used as model organisms to study the development of prostate cancer. As described previously, SPARC may be a molecular marker of developing tumors; thus, SPARC-binding peptide established to be SPPTGIN [106] was fused into pIII minor coat protein. At the same time, iron oxide nanoparticles' binding domain was fused into pVIII major coat in order to perform a visualization of cancer cells via MRI [107,108]. The result shows that biofunctionalized phages injected into an animal's bloodstream concentrate in regions of SPARC expression, enabling the recognition of prostate cancer tissue [107]. M13 bacteriophages are neutral for mammals and they can be injected into the bloodstream without serious disease or injury risk. Moreover, phages as naturally present entities in human intestines may get into the bloodstream and lymphatic reservoirs [9,11,109]. Some operations using M13 phages may be performed in vivo, e.g., the biopanning of the phage library was reviewed in detail [110,111]. The mentioned method is greatly expanded modification of panning procedure against eukaryotic cells [105]. Briefly, the peptide-phage library (pIII or pVIII) is injected into the bloodstream and, after the established time, the organ is resected, and binding phages are eluted and amplified. The in vivo panning method allows for selecting highly selective ligands resistant to interference from serum and intracellular fluid bio compounds. The experiments described above are usually conducted on model animals (e.g., mice), but experimental studies were performed on human organisms too [110,111]. These advanced studies directly connecting molecular biology (phage display) and modern medicine promise farther progress in phage-based imaging techniques.

5. Other Bacteriophages Applications

Apart from M13 bacteriophages, there are also other types of phages, e.g., T4, T7 or lambda phages, which were applied to generate random libraries [112–119]. Despite the advanced structure of these phages in comparison to filamentous phages libraries based on T4 and T7 have already been successfully applied for selecting several biomolecules, e.g., PSMA biomarker, which was reviewed previously [112–118].

A direct connection of phages with different transducers is usually performed for bacteria-sensor construction [29–32]. The application of a T4 phage in the sensor has the advantage of the ability to obtain a proper orientation of T4 in the electric field thanks to their nonzero permanent dipole moment [120]. The difference in charge distribution is different for head and tail. Thus, the head is partially negatively charged, while the tail, where the bacteria-binding receptors are localized, is positively charged. The immobilization of bacteriophages was conducted in the electric field (i.e., between covers of a capacitor, Figure 13) and enabled the immobilization of a higher density of phages with a proper orientation towards bacteria (Figure 14) [120]. Additionally, T4 virions might be genetically engineered to display desired binding motifs (e.g., selective for diseases biomarker) and the particles might be immobilized on a transducer in a proper orientation optimal for target binding.

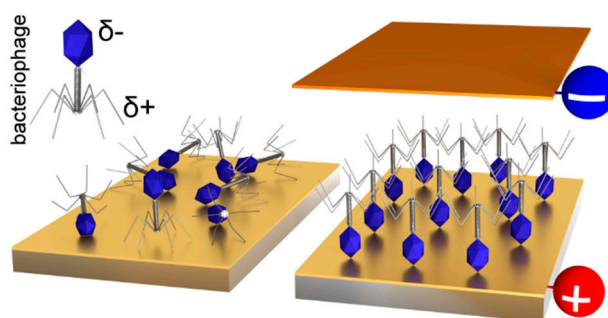


Figure 13. Scheme of the electric-field-dependent orientation of T4 bacteriophage. Without the electric field, phage orientation is random, but, if immobilization is conducted between capacitor covers, phages are generally oriented [120]. Reprinted from [120], Copyright 2016, with permission from Elsevier.

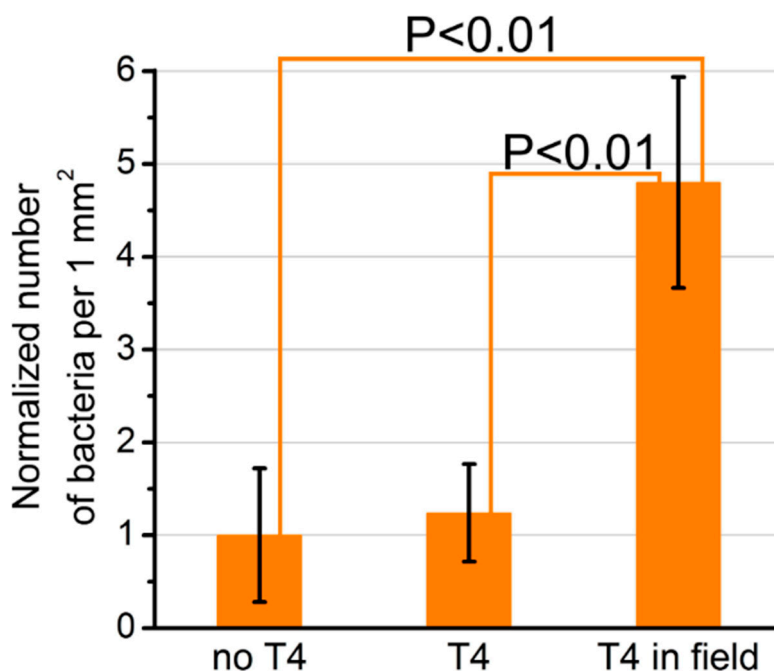


Figure 14. Conducting T4 bacteriophage immobilization in a constant external electric field enables a statistically significant higher phage density [120]. Reprinted from [120], Copyright 2016, with permission from Elsevier.

The genetic modification was also performed for T7 bacteriophages. As a result, genetically engineered phages display 15 amino acid along the epitope of West Nile virus (WNV) deriving

from the envelope protein of WNV [121]. The obtained epitope-carrying viruses were able to be detected via anti-WNV IgG antibodies and vice versa. This approach enabled the construction of a T7-based immunosensor for the detection of anti-WNV IgG antibodies [121]. As depicted in Figure 15, the sensor consists of a glassy carbon electrode modified with a receptor layer obtained via the electropolymerization of pyrrole-alkyl ammonium. The T7 phages were entrapped in the polymer layer and then the sensor was incubated with bovine serum albumin (BSA) solution in order to eliminate non-specific interactions. During sensor operation (schematically described in Figure 15), a sample containing anti-WNV IgG (or not) was incubated on the sensing layer and then the sensor was thoroughly rinsed with water. At the end, HRP-conjugated (horseradish peroxidase, HRP) anti-IgG antibodies were added. The sensing layer was washed and the amperometric measurements were performed, during which a product of enzymatic reaction oxidation, quinone, was reduced to hydroquinone, causing current flow observed as an analytical signal.

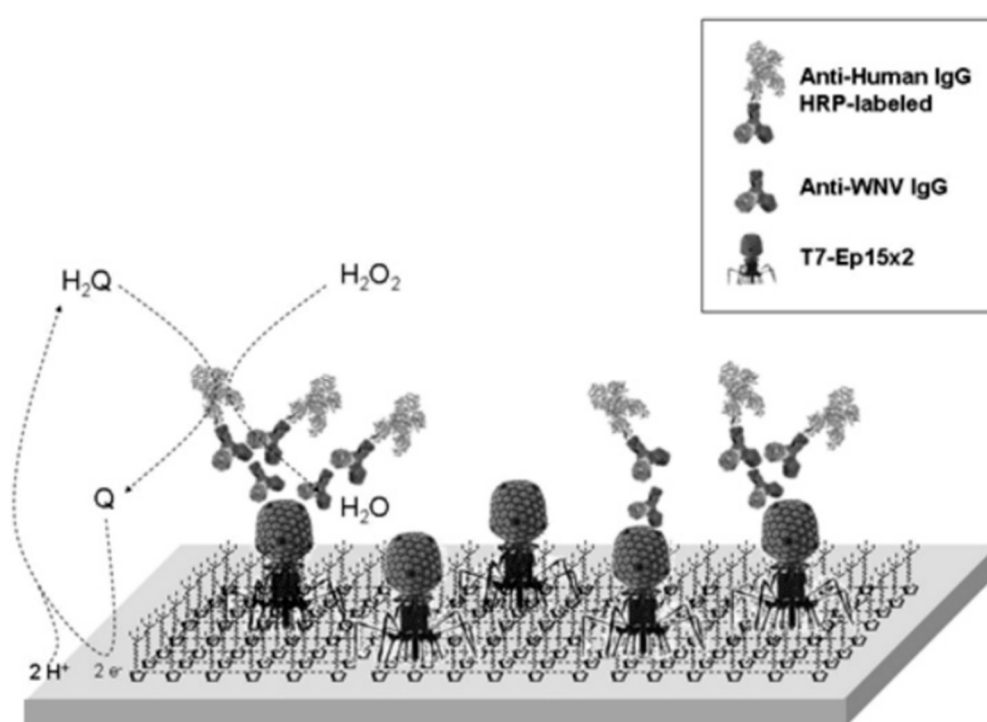


Figure 15. Scheme of T7 bacteriophage-based sensor for anti-WNV antibodies detection. WNV-epitope-carrying T7 phages are immobilized in the layer of conducting polymer. If the specific antibodies are present in the sample, they are bounded in a sandwich complex between a phage and a secondary antibody conjugated with an enzyme whose product is amperometrically detected [121]. Reprinted with permission from [121]. Copyright 2007 American Chemical Society.

The described assay requires multiple, laborious stages, and, besides, are a laboratory-usage technique only. Although these drawbacks, combining modified T7 bacteriophages with conductive polymer film may be in the future applied for construction of a novel, label-free and portable biosensors.

Filamentous bacteriophage f8-5 resembles M13 bacteriophages both in the case of genome and proteome [64]. Major coat protein pVIII of f8-5 phage exists in thousands of copies per virion and may be engineered similarly to M13 due to prepared landscape peptide library [64,119,122]. This type of library was utilized to select 8-mer peptide which selectively binds β -galactosidase. Further utilization of specific phage-based QCM and SPR biosensor was presented [64,119]. The receptor (phage carrying enzyme-binding peptide) showed a satisfying K_d at the level of 21 nM or 1.3 nM for the ELISA test and SPR sensor, respectively [64,119].

6. Summary

Bacteriophages are interesting entities at the border of chemistry and biology. Fundamental protein–protein interactions in phage particles are excellent examples of a combination of different molecular forces, e.g., van der Waals or hydrogen bonds, in living systems. The interactions are used in combination with genetically modified phages in the phage display technique to isolate selective ligands with nanomolar affinities for recognition of molecules, proteins or whole cells by their specific membrane receptors. Especially interesting are oligopeptides, which can be exposed on viral particles or chemically synthesized, because of their simplicity, easy handling and stability. The application of oligopeptides opens the door to develop novel sensing devices such as label-free *point-of-care* biosensors for detection of disease biomarkers or selective labeling systems for *in vivo* imaging. In the future, these peptides may be used as artificial antibodies. All of these advantages promise a continuation of the rapid progress in bacteriophage-based diagnostic tools observed already today. Although, there are no commercially available phage-based sensing devices, multiple technologies have been patented [123–126], which is promising for the future development of phage-based sensors.

Author Contributions: Conceptualization, S.J.M., K.S.-K., J.N.-J.; writing—original draft preparation, S.J.M.; writing—review and editing, S.J.M., K.S.-K., J.N.-J.; supervision, K.S.-K., J.N.-J. All authors have read and agreed to the published version of the manuscript.

Funding: This work has been financially supported by the Polish National Science Centre via a SONATA 13 grant UMO-2017/26/D/ST5/00980 to Katarzyna Szot-Karpińska and also by the 3/DOT/2016 project from the City of Gdynia.

Conflicts of Interest: The authors declare no conflict of interest.

References

1. Califf, R.M. Biomarker definitions and their applications. *Exp. Biol. Med.* **2018**, *243*, 213–221. [CrossRef]
2. Alpert, J.S.; Thygesen, K.; Antman, E.; Bassand, J.P. Myocardial infarction redefined—a consensus document of The Joint European Society of Cardiology/American College of Cardiology Committee for the redefinition of myocardial infarction. *J. Am. Coll. Cardiol.* **2000**, *36*, 959–969. [CrossRef]
3. Adigun, O.O.; Khetarpal, S. Alpha Fetoprotein (AFP, Maternal Serum Alpha Fetoprotein, MSAFP). In *StatPearls [Internet]*; StatPearls Publishing: Treasure Island, FL, USA, 2020. Available online: <https://www.ncbi.nlm.nih.gov/books/NBK430750/> (accessed on 24 July 2020).
4. Davies, R.J.; Eapen, S.S.; Carlisle, S.J. Lateral-Flow Immunochromatographic Assays. In *Handbook of Biosensors and Biochips*; Wiley-Interscience: Hoboken, NJ, USA, 2007.
5. Brigati, J.R.; Petrenko, V.A. Thermostability of landscape phage probes. *Anal. Bioanal. Chem.* **2005**, *382*, 1346–1350. [CrossRef]
6. Geysen, H.M.; Meloan, R.H.; Barteling, S.J. Use of peptide synthesis to probe viral antigens for epitopes to a resolution of a single amino acid. *Proc. Natl. Acad. Sci. USA* **1984**, *81*, 3998–4002. [CrossRef]
7. Smith, G.P. Filamentous fusion phage: Novel expression vectors that display cloned antigens on the virion surface. *Science* **1985**, *228*, 1315–1317. [CrossRef]
8. Clokie, M.R.; Millard, A.D.; Letarov, A.V.; Heaphy, S. Phages in nature. *Bacteriophage* **2011**, *1*, 31–45. [CrossRef]
9. Bakhshinejad, B.; Ghiasvand, S. Bacteriophages in the human gut: Our fellow travelers throughout life and potential biomarkers of health or disease. *Virus Res.* **2017**, *240*, 47–55. [CrossRef] [PubMed]
10. Salmond, G.P.C.; Fineran, P.C. A century of the phage: Past, present and future. *Nat. Rev. Microbiol.* **2015**, *13*, 777–786. [CrossRef] [PubMed]
11. Łusiak-Szelachowska, M.; Weber-Dąbrowska, B.; Jończyk-Matysiak, E.; Wojciechowska, R.; Górski, A. Bacteriophages in the gastrointestinal tract and their implications. *Gut Pathog.* **2017**, *9*, 1–5. [CrossRef] [PubMed]
12. Smith, G.P.; Petrenko, V.A. Phage display. *Chem. Rev.* **1997**, *97*, 391–410. [CrossRef] [PubMed]
13. Peltomaa, R.; Benito-Peña, E.; Barderas, R.; Moreno-Bondi, M.C. Phage display in the quest for new selective recognition elements for biosensors. *ACS Omega* **2019**, *4*, 11569–11580. [CrossRef] [PubMed]
14. Arnold, F.H. Directed Evolution: Bringing New Chemistry to Life. *Angew. Chem. Int. Ed.* **2018**, *57*, 4143–4148. [CrossRef] [PubMed]

15. Hentrich, C.; Ylera, F.; Frisch, C.; Ten Haaf, A.; Knappik, A. Chapter 3—Monoclonal Antibody Generation by Phage Display: History, State-of-the-Art, and Future. In *Handbook of Immunoassay Technologies*; Academic Press: Cambridge, MA, USA, 2018; pp. 47–80.
16. Bazan, J.; Całkosiński, I.; Gamian, A. Phage display—A powerful technique for immunotherapy. *Hum. Vaccines Immunother.* **2012**, *8*, 1817–1828. [[CrossRef](#)]
17. Ledsgaard, L.; Kilstrup, M.; Karatt-Vellatt, A.; McCafferty, J.; Laustsen, A.H. Basics of Antibody Phage Display Technology. *Toxins* **2018**, *10*, 236. [[CrossRef](#)]
18. Hammers, C.M.; Stanley, J.R. Antibody phage display: Technique and applications. *J. Investig. Dermatol.* **2014**, *134*, 1–5. [[CrossRef](#)]
19. Larman, H.B.; Zhao, Z.; Laserson, U.; Li, M.Z.; Ciccio, A.; Gakidis, M.A.M.; Church, G.M.; Kesari, S.; Leproust, E.M.; Solimini, N.L.; et al. Autoantigen discovery with a synthetic human peptidome. *Nat. Biotechnol.* **2011**, *29*, 535–541. [[CrossRef](#)]
20. Mimmi, S.; Maisano, D.; Quinto, I.; Iaccino, E. Phage Display: An Overview in Context to Drug Discovery. *Trends Pharmacol. Sci.* **2019**, *40*, 87–91. [[CrossRef](#)]
21. Hyde-Deruyser, R.; Paige, L.A.; Christensen, D.J.; Hyde-Deruyser, N.; Lim, A.; Fredericks, Z.L.; Kranz, J.; Gallant, P.; Zhang, J.; Rocklage, S.M.; et al. Detection of small-molecule enzyme inhibitors with peptides isolated from phage-displayed combinatorial peptide libraries. *Chem. Biol.* **2000**, *7*, 17–25. [[CrossRef](#)]
22. Park, I.W.; Kim, K.W.; Hong, Y.; Yoon, H.J.; Lee, Y.; Gwak, D.; Heo, K. Recent developments and prospects of M13-bacteriophage based piezoelectric energy harvesting devices. *Nanomaterials* **2020**, *10*, 93. [[CrossRef](#)] [[PubMed](#)]
23. Yang, S.H.; Chung, W.J.; McFarland, S.; Lee, S.W. Assembly of bacteriophage into functional materials. *Chem. Rec.* **2013**, *13*, 43–59. [[CrossRef](#)] [[PubMed](#)]
24. Janczuk, M.; Niedziółka-Jönsson, J.; Szot-Karpińska, K. Bacteriophages in electrochemistry: A review. *J. Electroanal. Chem.* **2016**, *779*, 207–219. [[CrossRef](#)]
25. Merzlyak, A.; Lee, S.W. Phage as templates for hybrid materials and mediators for nanomaterial synthesis. *Curr. Opin. Chem. Biol.* **2006**, *10*, 246–252. [[CrossRef](#)] [[PubMed](#)]
26. Mohan, K.; Weiss, G.A. Chemically Modifying Viruses for Diverse Applications. *ACS Chem. Biol.* **2016**, *11*, 1167–1179. [[CrossRef](#)] [[PubMed](#)]
27. Soto, C.M.; Ratna, B.R. Virus hybrids as nanomaterials for biotechnology. *Curr. Opin. Biotechnol.* **2010**, *21*, 426–438. [[CrossRef](#)] [[PubMed](#)]
28. Cui, Y. Engineered phages for electronics. *Biosens. Bioelectron.* **2016**, *85*, 964–976. [[CrossRef](#)]
29. Peltomaa, R.; López-Perolio, I.; Benito-Peña, E.; Barderas, R.; Moreno-Bondi, M.C. Application of bacteriophages in sensor development. *Anal. Bioanal. Chem.* **2016**, *408*, 1805–1828. [[CrossRef](#)]
30. Richter, Ł.; Janczuk-Richter, M.; Niedziółka-Jönsson, J.; Paczesny, J.; Hołyst, R. Recent advances in bacteriophage-based methods for bacteria detection. *Drug Discov. Today* **2018**, *23*, 448–455. [[CrossRef](#)]
31. Farooq, U.; Yang, Q.; Ullah, M.W.; Wang, S. Bacterial biosensing: Recent advances in phage-based bioassays and biosensors. *Biosens. Bioelectron.* **2018**, *118*, 204–216. [[CrossRef](#)]
32. Xu, J.; Chau, Y.; Lee, Y. kuen Phage-based electrochemical sensors: A review. *Micromachines* **2019**, *10*, 855. [[CrossRef](#)]
33. Adriaenssens, E.M.; Sullivan, M.B.; Knezevic, P.; van Zyl, L.J.; Sarkar, B.L.; Dutilh, B.E.; Alfenas-Zerbini, P.; Łobocka, M.; Tong, Y.; Brister, J.R.; et al. Taxonomy of prokaryotic viruses: 2018–2019 update from the ICTV Bacterial and Archaeal Viruses Subcommittee. *Arch. Virol.* **2020**, *165*, 1253–1260. [[CrossRef](#)]
34. Rakonjac, J.; Russel, M.; Khanum, S.; Brooke, S.J.; Rajic, M. Filamentous Phage: Structure and Biology. *Adv. Exp. Med. Biol.* **2017**, *1053*, 1–20. [[CrossRef](#)] [[PubMed](#)]
35. Marvin, D. Filamentous phage structure, infection and assembly. *Curr. Opin. Struct. Biol.* **1998**, *8*, 150–158. [[CrossRef](#)]
36. Russel, M. Moving through the membrane with filamentous phages. *Trends Microbiol.* **1995**, *3*, 223–228. [[CrossRef](#)]
37. Rakonjac, J.; Model, P. Roles of pIII in filamentous phage assembly. *J. Mol. Biol.* **1998**, *282*, 25–41. [[CrossRef](#)] [[PubMed](#)]
38. Weiss, G.A.; Roth, T.A.; Baldi, P.F.; Sidhu, S.S. Comprehensive mutagenesis of the C-terminal domain of the M13 gene-3 minor coat protein: The requirements for assembly into the bacteriophage particle. *J. Mol. Biol.* **2003**, *332*, 777–782. [[CrossRef](#)]

39. Specthrie, L.; Bullitt, E.; Horiuchi, K.; Model, P.; Russel, M.; Makowski, L. Construction of a microphage variant of filamentous bacteriophage. *J. Mol. Biol.* **1992**, *228*, 720–724. [[CrossRef](#)]
40. Qi, H.; Lu, H.; Qiu, H.J.; Petrenko, V.; Liu, A. Phagemid vectors for phage display: Properties, characteristics and construction. *J. Mol. Biol.* **2012**, *417*, 129–143. [[CrossRef](#)]
41. Grant, R.A.; Lin, T.C.; Konigsberg, W.; Webster, R.E. Structure of the Filamentous Bacteriophage f1. *J. Biol. Chem.* **1981**, *256*, 539–546.
42. Petrenko, V.A. Landscape phage: Evolution from phage display to nanobiotechnology. *Viruses* **2018**, *10*, 311. [[CrossRef](#)]
43. Cwirla, S.E.; Peters, E.A.; Barrett, R.W.; Dower, W.J. Peptides on phage: A vast library of peptides for identifying ligands. *Proc. Natl. Acad. Sci. USA* **1990**, *87*, 6378–6382. [[CrossRef](#)]
44. Noren, K.A.; Noren, C.J. Construction of high-complexity combinatorial phage display peptide libraries. *Methods* **2001**, *23*, 169–178. [[CrossRef](#)] [[PubMed](#)]
45. Cabilly, S. The basic structure of filamentous phage and its use in the display of combinatorial peptide libraries. *Appl. Biochem. Biotechnol. Part B Mol. Biotechnol.* **1999**, *12*, 143–148. [[CrossRef](#)]
46. Sidhu, S.S.; Lowman, H.B.; Cunningham, B.C.; Wells, J.A. Phage display for selection of novel binding peptides. *Methods Enzymol.* **2000**, *328*, 333–363. [[CrossRef](#)] [[PubMed](#)]
47. Sidhu, S.S. Engineering M13 for phage display. *Biomol. Eng.* **2001**, *18*, 57–63. [[CrossRef](#)]
48. Scott, J.K.; Smith, G.P. Searching for peptide ligands with an epitope library. *Science* **1990**, *249*, 386–390. [[CrossRef](#)] [[PubMed](#)]
49. Knez, K.; Noppe, W.; Geukens, N.; Janssen, K.P.F.; Spasic, D.; Heyligen, J.; Vriens, K.; Thevissen, K.; Cammue, B.P.A.; Petrenko, V.; et al. Affinity comparison of p3 and p8 peptide displaying bacteriophages using surface plasmon resonance. *Anal. Chem.* **2013**, *85*, 10075–10082. [[CrossRef](#)]
50. Friguet, B.; Chaffotte, A.F.; Djavadi-Ohanian, L.; Goldberg, M.E. Measurements of the true affinity constant in solution of antigen-antibody complexes by enzyme-linked immunosorbent assay. *J. Immunol. Methods* **1985**, *77*, 305–319. [[CrossRef](#)]
51. Park, J.P.; Crokek, D.M.; Banta, S. High affinity peptides for the recognition of the heart disease biomarker troponin I identified using phage display. *Biotechnol. Bioeng.* **2010**, *105*, 678–686. [[CrossRef](#)]
52. Petrenko, V.A.; Vodyanoy, V.J. Phage display for detection of biological threat agents. *J. Microbiol. Methods* **2003**, *53*, 253–262. [[CrossRef](#)]
53. Lim, J.M.; Kim, J.H.; Ryu, M.Y.; Cho, C.H.; Park, T.J.; Park, J.P. An electrochemical peptide sensor for detection of dengue fever biomarker NS1. *Anal. Chim. Acta* **2018**, *1026*, 109–116. [[CrossRef](#)]
54. Honegger, A. *Engineering Antibodies for Stability and Efficient Folding BT—Therapeutic Antibodies*; Chernajovsky, Y., Nissim, A., Eds.; Springer: Berlin/Heidelberg, Germany, 2008; pp. 47–68. ISBN 978-3-540-73259-4.
55. Yang, L.M.C.; Tam, P.Y.; Murray, B.J.; McIntire, T.M.; Overstreet, C.M.; Weiss, G.A.; Penner, R.M. Virus electrodes for universal biodetection. *Anal. Chem.* **2006**, *78*, 3265–3270. [[CrossRef](#)] [[PubMed](#)]
56. Mohan, K.; Donovan, K.C.; Arter, J.A.; Penner, R.M.; Weiss, G.A. Sub-nanomolar Detection of Prostate-Specific Membrane Antigen in Synthetic Urine by Synergistic, Dual-Ligand Phage. *J. Am. Chem. Soc.* **2013**, *135*, 7761–7767. [[CrossRef](#)] [[PubMed](#)]
57. Han, L.; Xia, H.; Yin, L.; Petrenko, V.A.; Liu, A. Selected landscape phage probe as selective recognition interface for sensitive total prostate-specific antigen immunosensor. *Biosens. Bioelectron.* **2018**, *106*, 1–6. [[CrossRef](#)] [[PubMed](#)]
58. Han, L.; Wang, D.; Yan, L.; Petrenko, V.A.; Liu, A. Specific phages-based electrochemical impedimetric immunosensors for label-free and ultrasensitive detection of dual prostate-specific antigens. *Sens. Actuators B Chem.* **2019**, *297*, 126727. [[CrossRef](#)]
59. Ogata, A.F.; Edgar, J.M.; Majumdar, S.; Briggs, J.S.; Patterson, S.V.; Tan, M.X.; Kudlacek, S.T.; Schneider, C.A.; Weiss, G.A.; Penner, R.M. Virus-Enabled Biosensor for Human Serum Albumin. *Anal. Chem.* **2017**, *89*, 1373–1381. [[CrossRef](#)] [[PubMed](#)]
60. Bhasin, A.; Ogata, A.F.; Briggs, J.S.; Tam, P.Y.; Tan, M.X.; Weiss, G.A.; Penner, R.M. The Virus Bioresistor: Wiring Virus Particles for the Direct, Label-Free Detection of Target Proteins. *Nano Lett.* **2018**, *18*, 3623–3629. [[CrossRef](#)]

61. Bhasin, A.; Sanders, E.C.; Ziegler, J.M.; Briggs, J.S.; Drago, N.P.; Attar, A.M.; Santos, A.M.; True, M.Y.; Ogata, A.F.; Yoon, D.V.; et al. Virus Bioresistor (VBR) for Detection of Bladder Cancer Marker DJ-1 in Urine at 10 pM in One Minute. *Anal. Chem.* **2020**, *92*, 6654–6666. [[CrossRef](#)]
62. Zhu, H.; White, I.M.; Suter, J.D.; Fan, X. Phage-based label-free biomolecule detection in an opto-fluidic ring resonator. *Biosens. Bioelectron.* **2008**, *24*, 461–466. [[CrossRef](#)]
63. Jia, Y.; Qin, M.; Zhang, H.; Niu, W.; Li, X.; Wang, L.; Li, X.; Bai, Y.; Cao, Y.; Feng, X. Label-free biosensor: A novel phage-modified Light Addressable Potentiometric Sensor system for cancer cell monitoring. *Biosens. Bioelectron.* **2007**, *22*, 3261–3266. [[CrossRef](#)]
64. Nanduri, V.; Balasubramanian, S.; Sista, S.; Vodyanoy, V.J.; Simonian, A.L. Highly sensitive phage-based biosensor for the detection of β -galactosidase. *Anal. Chim. Acta* **2007**, *589*, 166–172. [[CrossRef](#)]
65. Wu, J.; Crokek, D.M.; West, A.C.; Banta, S. Development of a troponin I biosensor using a peptide obtained through phage display. *Anal. Chem.* **2010**, *82*, 8235–8243. [[CrossRef](#)] [[PubMed](#)]
66. Wu, J.; Park, J.P.; Dooley, K.; Crokek, D.M.; West, A.C.; Banta, S. Rapid development of new protein biosensors utilizing peptides obtained via phage display. *PLoS ONE* **2011**, *6*. [[CrossRef](#)] [[PubMed](#)]
67. Hwang, H.J.; Ryu, M.Y.; Park, J.P. Identification of high affinity peptides for capturing norovirus capsid proteins. *RSC Adv.* **2015**, *5*, 55300–55302. [[CrossRef](#)]
68. Hwang, H.J.; Ryu, M.Y.; Park, C.Y.; Ahn, J.; Park, H.G.; Choi, C.; Ha, S.D.; Park, T.J.; Park, J.P. High sensitive and selective electrochemical biosensor: Label-free detection of human norovirus using affinity peptide as molecular binder. *Biosens. Bioelectron.* **2017**, *87*, 164–170. [[CrossRef](#)]
69. Padmanaban, G.; Park, H.; Choi, J.S.; Cho, Y.W.; Kang, W.C.; Moon, C.I.; Kim, I.S.; Lee, B.H. Identification of peptides that selectively bind to myoglobin by biopanning of phage displayed-peptide library. *J. Biotechnol.* **2014**, *187*, 43–50. [[CrossRef](#)]
70. Lee, H.Y.; Choi, J.S.; Guruprasath, P.; Lee, B.-H.; Cho, Y.W. An Electrochemical Biosensor Based on a Myoglobin-specific Binding Peptide for Early Diagnosis of Acute Myocardial Infarction. *Anal. Sci. Int. J. Jpn. Soc. Anal. Chem.* **2015**, *31*, 699–704. [[CrossRef](#)]
71. Park, J.P.; Park, C.Y.; Park, A.Y.; Ryu, M.Y. Evolutionary identification of affinity peptides for the detection of sepsis biomarker procalcitonin. *RSC Adv.* **2015**, *5*, 90531–90533. [[CrossRef](#)]
72. Lim, J.M.; Ryu, M.Y.; Kim, J.H.; Cho, C.H.; Park, T.J.; Park, J.P. An electrochemical biosensor for detection of the sepsis-related biomarker procalcitonin. *RSC Adv.* **2017**, *7*, 36562–36565. [[CrossRef](#)]
73. Lim, J.M.; Heo, N.S.; Oh, S.Y.; Ryu, M.Y.; Seo, J.H.; Park, T.J.; Huh, Y.S.; Park, J.P. Selection of affinity peptides for interference-free detection of cholera toxin. *Biosens. Bioelectron.* **2018**, *99*, 289–295. [[CrossRef](#)]
74. Cho, C.H.; Kim, J.H.; Song, D.K.; Park, T.J.; Park, J.P. An affinity peptide-incorporated electrochemical biosensor for the detection of neutrophil gelatinase-associated lipocalin. *Biosens. Bioelectron.* **2019**, *142*, 111482. [[CrossRef](#)]
75. Bravaccini, S.; Puccetti, M.; Bocchini, M.; Ravaioli, S.; Celli, M.; Scarpi, E.; De Giorgi, U.; Tumedei, M.M.; Raulli, G.; Cardinale, L.; et al. PSMA expression: A potential ally for the pathologist in prostate cancer diagnosis. *Sci. Rep.* **2018**, *8*, 1–8. [[CrossRef](#)] [[PubMed](#)]
76. Lisdat, F.; Schäfer, D. The use of electrochemical impedance spectroscopy for biosensing. *Anal. Bioanal. Chem.* **2008**, *391*, 1555–1567. [[CrossRef](#)] [[PubMed](#)]
77. Adams, J.E.; Bodor, G.S.; Davila-Roman, V.G.; Delmez, J.A.; Apple, F.S.; Ladenson, J.H.; Jaffe, A.S. Cardiac troponin I: A marker with high specificity for cardiac injury. *Circulation* **1993**, *88*, 101–106. [[CrossRef](#)] [[PubMed](#)]
78. Bagai, A.; Alexander, K.P.; Berger, J.S.; Senior, R.; Sajeev, C.; Pracon, R.; Mavromatis, K.; Lopez-Sendón, J.L.; Gosselin, G.; Diaz, A.; et al. Use of troponin assay 99th percentile as the decision level for myocardial infarction diagnosis. *Am. Heart J.* **2017**, *190*, 135–139. [[CrossRef](#)] [[PubMed](#)]
79. Gibler, W.B.; Gibler, C.D.; Weinshenker, E.; Abbottsmith, C.; Hedges, J.R.; Barsan, W.G.; Sperling, M.; Chen, I.W.; Embry, S.; Kereiakes, D. Myoglobin as an early indicator of acute myocardial infarction. *Ann. Emerg. Med.* **1987**, *16*, 851–856. [[CrossRef](#)]
80. Huang, X.-J.; Choi, Y.-K.; Im, H.-S.; Yarimaga, O.; Yoon, E.; Kim, H.-S. Aspartate Aminotransferase (AST/GOT) and Alanine Aminotransferase (ALT/GPT) Detection Techniques. *Sensors* **2006**, *6*, 756–782. [[CrossRef](#)]
81. Arter, J.A.; Taggart, D.K.; McIntire, T.M.; Penner, R.M.; Weiss, G.A. Virus-PEDOT nanowires for biosensing. *Nano Lett.* **2010**, *10*, 4858–4862. [[CrossRef](#)]

82. Donavan, K.C.; Arter, J.A.; Pilolli, R.; Cioffi, N.; Weiss, G.A.; Penner, R.M. Virus–Poly(3,4-ethylenedioxythiophene) Composite Films for Impedance-Based Biosensing. *Anal. Chem.* **2011**, *83*, 2420–2424. [[CrossRef](#)]
83. Arter, J.A.; Diaz, J.E.; Donavan, K.C.; Yuan, T.; Penner, R.M.; Weiss, G.A. Virus–Polymer Hybrid Nanowires Tailored to Detect Prostate-Specific Membrane Antigen. *Anal. Chem.* **2012**, *84*, 2776–2783. [[CrossRef](#)]
84. Donavan, K.C.; Arter, J.A.; Weiss, G.A.; Penner, R.M. Virus-PEDOT Biocomposite Films. *Langmuir* **2012**, *28*, 12581–12587. [[CrossRef](#)]
85. Saylan, Y.; Yilmaz, F.; Özgür, E.; Derazshamshir, A.; Bereli, N.; Yavuz, H.; Denizli, A. Surface Plasmon Resonance Sensors for Medical Diagnosis. In *Nanotechnology Characterization Tools for Biosensing and Medical Diagnosis*; Springer-Verlag GmbH: Heidelberg, Germany, 2018; pp. 425–458.
86. Dudak, F.C.; Boyaci, I.H. Rapid and label-free bacteria detection by surface plasmon resonance (SPR) biosensors. *Biotechnol. J.* **2009**, *4*, 1003–1011. [[CrossRef](#)] [[PubMed](#)]
87. Karoonuthaisiri, N.; Charlermroj, R.; Morton, M.J.; Oplatowska-Stachowiak, M.; Grant, I.R.; Elliott, C.T. Development of a M13 bacteriophage-based SPR detection using Salmonella as a case study. *Sens. Actuators B Chem.* **2014**, *190*, 214–220. [[CrossRef](#)]
88. Ding, X.; Yang, K.L. Development of an oligopeptide functionalized surface plasmon resonance biosensor for online detection of glyphosate. *Anal. Chem.* **2013**, *85*, 5727–5733. [[CrossRef](#)] [[PubMed](#)]
89. Pilot, R.; Signorini, R.; Durante, C.; Orian, L.; Bhamidipati, M.; Fabris, L. A review on surface-enhanced Raman scattering. *Biosensors* **2019**, *9*, 57. [[CrossRef](#)]
90. Moon, J.-S.; Kim, W.-G.; Kim, C.; Park, G.-T.; Heo, J.; Yoo, S.Y.; Oh, J.-W. M13 Bacteriophage-Based Self-Assembly Structures and Their Functional Capabilities. *Mini-Rev. Org. Chem.* **2015**, *12*, 271–281. [[CrossRef](#)]
91. Oh, J.W.; Chung, W.J.; Heo, K.; Jin, H.E.; Lee, B.Y.; Wang, E.; Zueger, C.; Wong, W.; Meyer, J.; Kim, C.; et al. Biomimetic virus-based colourimetric sensors. *Nat. Commun.* **2014**, *5*, 1–8. [[CrossRef](#)]
92. Moon, J.S.; Lee, Y.; Shin, D.M.; Kim, C.; Kim, W.G.; Park, M.; Han, J.; Song, H.; Kim, K.; Oh, J.W. Identification of Endocrine Disrupting Chemicals using a Virus-Based Colorimetric Sensor. *Chem. Asian J.* **2016**, *11*, 3097–3101. [[CrossRef](#)]
93. Kim, W.G.; Song, H.; Kim, C.; Moon, J.S.; Kim, K.; Lee, S.W.; Oh, J.W. Biomimetic self-templating optical structures fabricated by genetically engineered M13 bacteriophage. *Biosens. Bioelectron.* **2016**, *85*, 853–859. [[CrossRef](#)]
94. Moon, J.S.; Park, M.; Kim, W.G.; Kim, C.; Hwang, J.; Seol, D.; Kim, C.S.; Sohn, J.R.; Chung, H.; Oh, J.W. M-13 bacteriophage based structural color sensor for detecting antibiotics. *Sens. Actuators B Chem.* **2017**, *240*, 757–762. [[CrossRef](#)]
95. Moon, J.S.; Kim, W.G.; Shin, D.M.; Lee, S.Y.; Kim, C.; Lee, Y.; Han, J.; Kim, K.; Yoo, S.Y.; Oh, J.W. Bioinspired M-13 bacteriophage-based photonic nose for differential cell recognition. *Chem. Sci.* **2017**, *8*, 921–927. [[CrossRef](#)]
96. Moon, J.S.; Choi, J.; Hwang, Y.H.; Oh, J.W. Liquid Sensing of a M-13 Bacteriophage-Based Colorimetric Sensor. *Macromol. Res.* **2018**, *26*, 775–779. [[CrossRef](#)]
97. Tronolone, J.J.; Orrill, M.; Song, W.; Kim, H.S.; Lee, B.Y.; Leblanc, S. Electric field assisted self-assembly of viruses into colored thin films. *Nanomaterials* **2019**, *9*, 1310. [[CrossRef](#)] [[PubMed](#)]
98. Kim, C.; Lee, H.; Devaraj, V.; Kim, W.G.; Lee, Y.; Kim, Y.; Jeong, N.N.; Choi, E.J.; Baek, S.H.; Han, D.W.; et al. Hierarchical cluster analysis of medical chemicals detected by a bacteriophage-based colorimetric sensor array. *Nanomaterials* **2020**, *10*, 121. [[CrossRef](#)] [[PubMed](#)]
99. Chung, W.J.; Oh, J.W.; Kwak, K.; Lee, B.Y.; Meyer, J.; Wang, E.; Hexemer, A.; Lee, S.W. Biomimetic self-templating supramolecular structures. *Nature* **2011**, *478*, 364–368. [[CrossRef](#)]
100. Zhu, H.; White, I.M.; Suter, J.D.; Zourob, M.; Fan, X. Opto-fluidic micro-ring resonator for sensitive label-free viral detection. *Analyst* **2008**, *133*, 356–360. [[CrossRef](#)] [[PubMed](#)]
101. Suter, J.D.; Fan, X. Overview of the optofluidic ring resonator: A versatile platform for label-free biological and chemical sensing. In *Proceedings of the 31st Annual International Conference of the IEEE Engineering in Medicine and Biology Society: Engineering the Future of Biomedicine, EMBC, Minneapolis, MN, USA, 3–6 September 2009*; pp. 1042–1044. [[CrossRef](#)]
102. Chen, L.; Zurita, A.J.; Ardelt, P.U.; Giordano, R.J.; Arap, W.; Pasqualini, R. Design and validation of a bifunctional ligand display system for receptor targeting. *Chem. Biol.* **2004**, *11*, 1081–1091. [[CrossRef](#)]
103. Kim, I.; Moon, J.-S.; Oh, J.-W. Recent advances in M13 bacteriophage-based optical sensing applications. *Nano Converg.* **2016**, *3*. [[CrossRef](#)]

104. Sun, Y.; Shukla, G.S.; Weaver, D.; Pero, S.C.; Krag, D.N. Phage-display selection on tumor histological specimens with laser capture microdissection. *J. Immunol. Methods* **2009**, *347*, 46–53. [[CrossRef](#)]
105. Xu, H.; Cao, B.; Li, Y.; Mao, C. Phage nanofibers in nanomedicine: Biopanning for early diagnosis, targeted therapy, and proteomics analysis. *Wiley Interdiscip. Rev. Nanomed. Nanobiotechnol.* **2020**, 1–33. [[CrossRef](#)]
106. Kelly, K.A.; Waterman, P.; Weissleder, R. In vivo imaging of molecularly targeted phage. *Neoplasia* **2006**, *8*, 1011–1018. [[CrossRef](#)]
107. Ghosh, D.; Lee, Y.; Thomas, S.; Kohli, A.G.; Yun, D.S.; Belcher, A.M.; Kelly, K.A. M13-templated magnetic nanoparticles for targeted in vivo imaging of prostate cancer. *Nat. Nanotechnol.* **2012**, *7*, 677–682. [[CrossRef](#)]
108. Park, J.; An, K.; Hwang, Y.; Park, J.E.G.; Noh, H.J.; Kim, J.Y.; Park, J.H.; Hwang, N.M.; Hyeon, T. Ultra-large-scale syntheses of monodisperse nanocrystals. *Nat. Mater.* **2004**, *3*, 891–895. [[CrossRef](#)]
109. Krut, O.; Bekeredian-Ding, I. Contribution of the Immune Response to Phage Therapy. *J. Immunol.* **2018**, *200*, 3037–3044. [[CrossRef](#)]
110. Bábícková, J.; Tóthová, L.; Boor, P.; Celec, P. In vivo phage display—A discovery tool in molecular biomedicine. *Biotechnol. Adv.* **2013**, *31*, 1247–1259. [[CrossRef](#)]
111. Trepel, M.; Arap, W.; Pasqualini, R. In vivo phage display and vascular heterogeneity: Implications for targeted medicine. *Curr. Opin. Chem. Biol.* **2002**, *6*, 399–404. [[CrossRef](#)]
112. Deng, X.; Wang, L.; You, X.; Dai, P.; Zeng, Y. Advances in the T7 phage display system (Review). *Mol. Med. Rep.* **2018**, *17*, 714–720. [[CrossRef](#)]
113. Nicastro, J.; Sheldon, K.; Slavcev, R.A. Bacteriophage lambda display systems: Developments and applications. *Appl. Microbiol. Biotechnol.* **2014**, *98*, 2853–2866. [[CrossRef](#)]
114. Gamkrelidze, M.; Dąbrowska, K. T4 bacteriophage as a phage display platform. *Arch. Microbiol.* **2014**, *196*, 473–479. [[CrossRef](#)]
115. Sharma, S.C.; Memic, A.; Rupasinghe, C.N.; Duc, A.C.E.; Spaller, M.R. T7 phage display as a method of peptide ligand discovery for PDZ domain proteins. *Biopolymers* **2009**, *92*, 183–193. [[CrossRef](#)]
116. Maruyama, I.N.; Maruyama, H.I.; Brenner, S. λ foo: A λ phage vector for the expression of foreign proteins. *Proc. Natl. Acad. Sci. USA* **1994**, *91*, 8273–8277. [[CrossRef](#)]
117. van Wezenbeek, P.M.; Hulsebos, T.J.; Schoenmakers, J.G. Nucleotide sequence of the filamentous bacteriophage M13 DNA genome: Comparison with phage fd. *Gene* **1980**, *11*, 129–148. [[CrossRef](#)]
118. Sternberg, N.; Hoess, R.H. Display of peptides and proteins on the surface of bacteriophage λ . *Proc. Natl. Acad. Sci. USA* **1995**, *92*, 1609–1613. [[CrossRef](#)] [[PubMed](#)]
119. Nanduri, V.; Sorokulova, I.B.; Samoylov, A.M.; Simonian, A.L.; Petrenko, V.A.; Vodyanoy, V. Phage as a molecular recognition element in biosensors immobilized by physical adsorption. *Biosens. Bioelectron.* **2007**, *22*, 986–992. [[CrossRef](#)] [[PubMed](#)]
120. Richter, Ł.; Matuła, K.; Leśniewski, A.; Kwaśnicka, K.; Łoś, J.; Łoś, M.; Paczesny, J.; Hołyst, R. Ordering of bacteriophages in the electric field: Application for bacteria detection. *Sens. Actuators B Chem.* **2016**, *224*, 233–240. [[CrossRef](#)]
121. Ionescu, R.E.; Cosnier, S.; Herrmann, S.; Marks, R.S. Amperometric immunosensor for the detection of anti-West Nile virus IgG. *Anal. Chem.* **2007**, *79*, 8662–8668. [[CrossRef](#)] [[PubMed](#)]
122. Petrenko, V.A.; Smith, G.P.; Gong, X.; Quinn, T. A library of organic landscapes on filamentous phage. *Protein Eng. Des. Sel.* **1996**, *9*, 797–801. [[CrossRef](#)]
123. Evoy, S.; Singh, A.; Glass, N. Bacteriophage Immobilization for Biosensors. U.S. Patent 2010/0291541 A1, 18 November 2010.
124. Ramasamy, R.P.; Zhou, Y. Bacteriophage-Based Electrochemical Bacterial Sensors, Systems, and Methods. U.S. Patent 2020/0033340 A1, 30 January 2020.
125. Albrecht, J.; Conrad, A.J. Biologic Machines for the Detection of Biomolecules. U.S. Patent 10,662,459 B2, 26 May 2020.
126. Weiss, G.A.; Penner, R.M.; Tam, P.Y.; Yang, L.-M.; Brigham, T. Method and Apparatus for Target Detection Using Electrode-Bound Viruses. U.S. Patent 8,513,001 B2, 20 August 2013.

